APPENDIX

SUPPLEMENTARY MATERIAL

CHAPTER 1

Experimental Procedures:

I. **Recording the thermal anomaly**

HOBO temperature loggers deployed underwater at each of the study sites in Puerto Rico had been recording water temperatures every two hours since 2003, providing information on the temperature conditions and variability before, during and after the thermal anomaly. The presence of a thermal anomaly was corroborated using NOAA Coral Reef Watch: http://coralreefwatch.noaa.gov/satellite/index.php.

II. **Sample collection**

Samples of *G. ventalina* were collected at Laurel Patch (17° 56.480 N and 67° 04.484 W) in La Parguera, PR. Samples of *O. faveolata* were collected at Media Luna reef (17° 56.096' N, 67° 02.911' W). Each sample was placed in a sterilized bag, stored on ice for transport to the lab, and drained of excess seawater before flash-freezing in liquid nitrogen and shipping on dry ice.

III. **DNA extraction**

We extracted microbial DNA from whole organism samples of both coral species because coral tissue, mucus and skeleton provide unique habitats due to their chemical and physical properties (Sharp et al., 2012; Rosenberg et al., 2007). 1x2 cm of frozen tissue from the whole organism was ground to a powder in liquid nitrogen with a sterilized mortar and pestle. The optimal starting quantities were 100 mg of *G. ventalina* and 200 mg of *O. faveolata*. We added the samples to PowerSoil DNA Isolation Kit (MoBio Laboratories) bead tubes, then stored them at -80°C. We modified the kit protocol to improve quality and yield as per Sunagawa et al., 2010: 1) incubation with 10 U μL^{-1} lysozyme (0.19µL; Epicentre) for 10 min at room temperature; 2) incubation with ~0.8 mg mL^{-1} proteinase K (25µL; Invitrogen) for 60 min at 65°C; 3) addition of 400 mg each of 0.1 and 0.5 mm zirconia/silica beads; and 4) homogenization for 30 s at 30 beats/s (Retsch MM300 Bead Beater). Total genomic DNA concentrations were determined using the Quant-iT PicoGreen dsDNA Assay kit (Invitrogen).

IV. **16S rRNA Amplicon Generation, Quantification, Pooling and 454 Pyrosequencing**

Approximately 14 ng (~1-5 µl) of template DNA was used in each of three replicate, 30 µl PCR reactions with Taq DNA Polymerase (Invitrogen). PCR cycling conditions and primers are described below. The reactions were pooled and run on a 2% Agarose-TAE gel to confirm products. The pooled products were then purified with Ampure magnetic purification beads (Agencourt) and quantified using the Quant-

iT PicoGreen dsDNA Assay kit (Invitrogen). Pooled samples were sent to Engencore (University of South Carolina) for pyrosequencing using Roche 454 with Titanium and FLX platforms. Sequences were submitted to NCBI's Sequence Read Archive under SRP052076: http://www.ncbi.nlm.nih.gov/bioproject/270509

Cylcing conditions: 94°C-2', [94°C-30", 53°C-45", 72°C-1'] x30, 72°C-10'
Primers:

We used the forward primer 5′-*GCCTTGCCAGCCCGCTCAGTC* **AGAGTTTGATCCTGGCTCAG**-3′: the italicized sequence is 454 Life Sciences primer B, and the bold sequence is the broadly conserved bacterial primer 27F. The reverse primer used was 5′-*GCCTCCCTCGCGCCATCAGNNNNNNNNNNNNCA* **TGCTGCCTCCCGTAGGAGT**-3′: the italicized sequence is 454 Life Sciences primer A. The bold sequence is the broad-range bacterial primer 338R. *NNNNNNNNNNN* designates the unique 12-base barcode used to tag each PCR product, with "CA" inserted as a linker between the barcode and rRNA gene primer (Hamady et al., 2008; Koren et al., 2011).

V. **Analysis of Sequence Data**

Sequences were checked for chimeras using UCHIME and assigned to OTUs using OTUpipe (Edgar et al., 2011) with a 97% threshold of pairwise identity, and then classified taxonomically using the Greengenes reference database (McDonald et al., 2012). For quality filtering, the following sequences were discarded: <200 bp or >1,000 bp, and sequences containing >0 primer mismatches, uncorrectable barcodes, >0 ambiguous bases, or homopolymer runs in excess of 6 bases.

VI. **Statistical Analyses**

We tested sampling time, coral species, and *Symbiodinium* density (for *O. faveolata*) as predictors of the microbiota using adonis with 1000 permutations (Oksanen et al., 2013). For *G. ventalina*, pairwise comparisons tested for significant shifts between adjacent sampling times, yielding FDR-corrected p values (q values) with padjust. The association of OTUs with sampling times, host species, and *Symbiodinium* densities, and thus their contributions to distinct microbiota, was determined with indicspecies (De Caceres et al., 2009).

We used QIIME and the Shannon diversity index to make rarefaction plots of alpha diversity (Figures S1, S2, and S3). A generalized linear model (GLM) with the Gamma distribution (R Core Team, 2012) and pairwise comparisons using multcomp (Oksanen et al., 2013) were used to test sampling time and coral host as predictors of alpha diversity.

GLMs on select taxa over time were conducted in R (Table S1). We used the negative binomial distribution for GLMs because it is appropriate for count data where the variance is high relative to the mean (Crawley, 2007). We used glm.nb to test the effect of timing in *O. faveolata* (Venables et al., 2002) and mixed effects GLMs (glmer.nb) to address pseudosampling in *G. ventalina* with timing as a fixed effect and

colony as a random effect (Bates et al., 2012). The Akaike information criterion (AIC) determined the selection of the best-fit model. FDR corrections were applied to the *G. ventalina* and *O. faveolata* models to account for multiple tests using the p.adjust command in R.

Independent *a priori* contrasts for *G. ventalina* encode the following pairwise comparisons: before vs. during the 2010 warming event, during vs. Recovery 1, and Recovery 1 vs. Recovery 2.
For *O. faveolata*, with only three total sampling times, the *a priori* contrasts were: during vs. Recovery 2 and Recovery 1 vs. Recovery 2.

VII. Analyses of OTUs and higher taxa

Table S1.1. The select higher taxa analyzed in GLMs for *G. ventalina* (GV) and *O. faveolata* (OF). These taxa were selected based on the overall abundance in our data and biological associations from past studies. The rank abundances are taken from a rarefied OTU table that standardizes the OTUs in each sample.

Focal taxon	GLM on taxon	Coral literature: Biological associations
PHYLA		
Bacteroidetes	Yes	Diseased (Bourne 2013; Pantos and Bythell 2006; Webster et al. 2008; Vega Thurber et al. 2009; Roder et al. 2013b); Healthy (Roder et al. 2013; Kellogg et al. 2013)
Acidobacter	Yes	Bleached (Mouchka et al. 2010); Healthy (Chen et al. 2011)
Cyanobacteria	Yes	Diseased (Sato 2009; Mouchka et al. 2010; Kellogg et al. 2013); Healthy (Vega Thurber 2009; Kimes et al. 2013; Littman 2011)
CLASSES		
Gamma-proteobacteria (Class)	Yes	Diseased (Roder et al. 2013); Bleached (Koren et al. 2008; Lins-de-Barros et al. 2013); Cave corals (Koren et al. 2008); Healthy (Lee et al. 2012; La Riviere et al. 2013; Kimes et al. 2013; Sharp et al. 2012; Roder et al. 2013)
Alpha-proteobacteria (Class)	Yes	Diseased (Roder et al. 2013; Kellogg et al. 2013); Bleached and cave corals (Koren et al. 2008; Lins-de-Barros et al. 2013); Healthy (Koren et al. 2006; Kvennefors 2012; Ritchie 2011, Kimes et al. 2013); Healthy and diseased, different ribotypes in each (Pantos et al. 2003)
Delta-proteobacteria (Class)	No because of low sequence counts	Diseased (Bourne 2013- review citing (Frias-Lopez et al. 2002; Pantos and Bythell 2006; Webster et al. 2008)

Clostridia (Class)	Yes	Diseased (Mouchka et al. 2010; Kellogg et al. 2013; Roder et al. 2013); Healthy (Littman et al. 2011; Kellogg et al. 2013; Kimes et al. 2013; Roder et al. 2013)
ORDERS		
Oceano-spirillales (Order)	Yes	Diseased (Roder et al. 2013; Kellogg et al. 2013); Healthy (La Riviere et al. 2013; Mouchka et al. 2010)
FAMILIES		
Pseudo-monadaceae (Family)	Yes	Healthy (McGrath and Smith, 1999; Koren et al. 2006; Ritchie et al. 1994)
Vibrionaceae (Family)	No because of low sequence counts	Diseased (Bourne 2008; Sunagawa 2010, 2009; Roder et al. 2013; Garcia et al., 2013); Healthy (Koren et al. 2006; Raina et al. 2009; Kellogg et al. 2013); Bleached, healthy, and cave corals (Koren et al. 2008); Bleached (Ritchie et al. 1994); Bleached/ Diseased (Rubio et al. 2013)
Rhodo-bacteraceae (Family)	Yes	Diseased (Sunagawa 2009; Roder et al. 2013; Kellogg et al. 2013; Mouchka et al. 2010); Healthy (Koren et al. 2006)
Rickettsiaceae (Family)	Yes	Diseased, White Plague (Garcia et al. 2013); Healthy and Diseased (Casas et al., 2004)

VIII. Image processing and preparation

All images were constructed using Adobe Illustrator CS6 using output files directly from QIIME (beta_diversity_through_plots.py and summarize_taxa.py). Images were edited for orientation, correct file format, and to include color legends.

Results:

Table S1.2: Results of indicspecies analysis for *G. ventalina* vs. *O. faveolata*

OTU	Group Association	p value	Taxonomy
OTU_97.1254	*O. faveolata*	0.002	Root; k__Bacteria; p__Proteobacteria; c__Alphaproteobacteria; o__Rhodobacterales; f__Rhodobacteraceae; g__Ruegeria; Unclassified_subdomains; otu_2655
OTU_97.860	*O. faveolata*	0.003	Root; k__Bacteria; p__Proteobacteria; c__Alphaproteobacteria; o__Rhodobacterales; f__Rhodobacteraceae

OTU_97.97	*O. faveolata*	0.005	Root; k__Bacteria; p__Proteobacteria; c__Gammaproteobacteria; o__Vibrionales; f__Vibrionaceae
OTU_97.13	*O. faveolata*	0.006	Root; k__Bacteria; p__Bacteroidetes; c__Sphingobacteria; o__Sphingobacteriales; f__Flammeovirgaceae; Unclassified_subdomains; otu_1173
OTU_97.91	*O. faveolata*	0.007	Root; k__Bacteria; p__Verrucomicrobia; c__Verrucomicrobiae; o__Verrucomicrobiales; f__Verrucomicrobiaceae; g__Rubritalea; otu_4261
OTU_97.72	*O. faveolata*	0.008	Root; k__Bacteria; p__Proteobacteria; c__Alphaproteobacteria
OTU_97.1078	*O. faveolata*	0.015	Root; k__Bacteria
OTU_97.241	*O. faveolata*	0.019	Root; k__Bacteria; p__Bacteroidetes; c__Flavobacteria; o__Flavobacteriales; f__Flavobacteriaceae; g__Tenacibaculum
OTU_97.432	*O. faveolata*	0.019	Root; k__Bacteria
OTU_97.73	*O. faveolata*	0.02	Root; k__Bacteria; p__Proteobacteria; c__Alphaproteobacteria; o__Rhizobiales; f__Rhodobacteraceae; g__Labrenzia; s__Labrenzia_aggregata
OTU_97.1387	*O. faveolata*	0.024	Root; k__Bacteria
OTU_97.226	*O. faveolata*	0.025	Root; k__Bacteria; p__Proteobacteria; c__Gammaproteobacteria; o__Thiotrichales; f__Francisellaceae; g__Francisella; Unclassified_subdomains; otu_3834
OTU_97.743	*O. faveolata*	0.025	Root; k__Bacteria; p__Chloroflexi; c__Anaerolineae; o__S0208; otu_1308
OTU_97.59	*O. faveolata*	0.029	Root; k__Bacteria; p__Proteobacteria; c__Betaproteobacteria; o__Burkholderiales; f__Oxalobacteraceae; g__Massilia; s__Massilia_timonae
OTU_97.1407	*O. faveolata*	0.031	Root; k__Bacteria
OTU_97.710	*O. faveolata*	0.032	Root; k__Bacteria; p__Cyanobacteria; c__Chloroplast; o__; f__; g__CAB-I; otu_1354
OTU_97.209	*O. faveolata*	0.035	Root; k__Bacteria
OTU_97.842	*O. faveolata*	0.036	Root; k__Bacteria; p__Firmicutes
OTU_97.50	*O. faveolata*	0.039	Root; k__Bacteria; p__Bacteroidetes; c__Flavobacteria; o__Flavobacteriales; f__Flavobacteriaceae; g__Tenacibaculum; Unclassified_subdomains; otu_1136
OTU_97.109	*O. faveolata*	0.041	Root; k__Bacteria; p__Proteobacteria; c__Alphaproteobacteria; o__Rhizobiales;

			f__Rhodobacteraceae; g__Labrenzia; s__Labrenzia_aggregata
OTU_97.308	*O. faveolata*	0.042	Root; k__Bacteria; p__Bacteroidetes; c__Sphingobacteria; o__Sphingobacteriales; f__; Unclassified_subdomains; otu_1153
OTU_97.960	*O. faveolata*	0.044	Root; k__Bacteria
OTU_97.2157	*O. faveolata*	0.045	Root; k__Bacteria
OTU_97.1822	*O. faveolata*	0.048	Root; k__Bacteria
OTU_97.483	*O. faveolata*	0.049	Root; k__Bacteria; p__Cyanobacteria; c__Chloroplast; o__Stramenopiles; otu_1367
OTU_97.433	*O. faveolata*	0.05	Root; k__Bacteria; p__Firmicutes; c__Clostridia; o__Clostridiales; f__Clostridiaceae; g__Clostridium
OTU_97.3	*G. ventalina*	0.001	Root; k__Bacteria
OTU_97.111	*G. ventalina*	0.001	Root; k__Bacteria; p__Firmicutes; c__Clostridia; o__Natranaerobiales; f__ML1228J-1; otu_2205
OTU_97.351	*G. ventalina*	0.002	Root; k__Bacteria; p__Bacteroidetes; c__; o__; f__; Unclassified_subdomains; otu_966
OTU_97.35	*G. ventalina*	0.002	Root; k__Bacteria; p__Firmicutes; c__Clostridia; o__Halanaerobiales; f__Halanaerobiaceae; Unclassified_subdomains; otu_2189
OTU_97.88	*G. ventalina*	0.003	Root; k__Bacteria; p__Firmicutes; c__Clostridia; o__Clostridiales; f__Peptococcaceae; g__Desulfotomaculum; Unclassified_subdomains; otu_2093
OTU_97.2238	*G. ventalina*	0.004	Root; k__Bacteria; p__Proteobacteria
OTU_97.1068	*G. ventalina*	0.005	Root; k__Bacteria; p__Bacteroidetes; c__; o__; f__; Unclassified_subdomains; otu_966
OTU_97.1590	*G. ventalina*	0.007	Root; k__Bacteria; p__Bacteroidetes; c__; o__; f__; Unclassified_subdomains; otu_966
OTU_97.1416	*G. ventalina*	0.008	Root; k__Bacteria; p__Bacteroidetes; c__; o__; f__; Unclassified_subdomains; otu_966
OTU_97.251	*G. ventalina*	0.01	Root; k__Bacteria; p__Bacteroidetes; c__Bacteroidia; o__Bacteroidales; f__Bacteroidaceae; g__Bacteroides; s__Bacteroides_uniformis
OTU_97.137	*G. ventalina*	0.012	Root; k__Bacteria; p__Firmicutes; c__Clostridia; o__Clostridiales; f__Clostridiaceae; Unclassified_subdomains; otu_1949
OTU_97.132	*G. ventalina*	0.016	Root; k__Bacteria; p__Firmicutes
OTU_97.85	*G. ventalina*	0.018	Root; k__Bacteria; p__Bacteroidetes; c__; o__; f__; g__Candidatus_Cardinium
OTU_97.590	*G. ventalina*	0.02	Root; k__Bacteria; p__Firmicutes; c__Clostridia; o__Clostridiales; f__Catabacteriaceae; otu_1948

OTU_97.2116	*G. ventalina*	0.021	Root; k__Bacteria; p__Bacteroidetes; c__Sphingobacteria; o__Sphingobacteriales; f__Flammeovirgaceae; Unclassified_subdomains; otu_1173
OTU_97.2106	*G. ventalina*	0.026	Root; k__Bacteria; p__Bacteroidetes
OTU_97.84	*G. ventalina*	0.028	Root; k__Bacteria; p__Chloroflexi; c__Chloroflexi_(class); o__Chloroflexales; f__Chlorothrixaceae; otu_1320
OTU_97.22	*G. ventalina*	0.03	Root; k__Bacteria; p__Bacteroidetes; c__Sphingobacteria; o__Sphingobacteriales; f__Flammeovirgaceae; Unclassified_subdomains; otu_1173
OTU_97.134	*G. ventalina*	0.031	Root; k__Bacteria; p__Proteobacteria; c__Alphaproteobacteria
OTU_97.212	*G. ventalina*	0.031	Root; k__Bacteria; p__Bacteroidetes; c__Bacteroidia; o__Bacteroidales; Unclassified_subdomains; otu_973
OTU_97.1115	*G. ventalina*	0.034	Root; k__Bacteria; p__Firmicutes; c__Clostridia; o__Natranaerobiales; f__ML1228J-1; otu_2205
OTU_97.554	*G. ventalina*	0.035	Root; k__Bacteria; p__Firmicutes; c__Clostridia; o__Halanaerobiales; f__Halanaerobiaceae; Unclassified_subdomains; otu_2189
OTU_97.143	*G. ventalina*	0.038	Root; k__Bacteria; p__Bacteroidetes; c__Flavobacteria
OTU_97.197	*G. ventalina*	0.038	Root; k__Bacteria
OTU_97.815	*G. ventalina*	0.041	Root; k__Bacteria; p__Bacteroidetes; c__Flavobacteria; o__Flavobacteriales; f__Flavobacteriaceae
OTU_97.58	*G. ventalina*	0.044	Root; k__Bacteria; p__Spirochaetes; c__Spirochaetes_(class); o__Spirochaetales; f__Spirochaetaceae; Unclassified_subdomains; otu_3973
OTU_97.258	*G. ventalina*	0.048	Root; k__Bacteria; p__Bacteroidetes; c__Bacteroidia; o__Bacteroidales; Unclassified_subdomains; otu_973
OTU_97.582	*G. ventalina*	0.05	Root; k__Bacteria; p__Spirochaetes; c__Spirochaetes_(class); o__Spirochaetales; f__Spirochaetaceae; Unclassified_subdomains; otu_3973

Table S1.3: Results of indicspecies analysis for *G. ventalina* by sampling time

OTU	**Group Association**	**p value**	**Taxonomy**
OTU_97.112	Before	0.001	Root; k__Bacteria; p__Bacteroidetes; c__Bacteroidia; o__Bacteroidales; Unclassified_subdomains; otu_973

OTU_97.61	Before	0.001	Root; k__Bacteria; p__Cyanobacteria; c__Synechococcophycideae; o__Synechococcales; f__Synechococcaceae; g__Prochlorococcus; otu_1472
OTU_97.251	Before	0.001	Root; k__Bacteria; p__Bacteroidetes; c__Bacteroidia; o__Bacteroidales; f__Bacteroidaceae; g__Bacteroides; s__Bacteroides_uniformis
OTU_97.223	Before	0.001	Root; k__Bacteria; p__Bacteroidetes; c__Bacteroidia; o__Bacteroidales; Unclassified_subdomains; otu_973
OTU_97.203	Before	0.001	Root; k__Bacteria; p__Firmicutes; c__Clostridia; o__Clostridiales; f__Lachnospiraceae; g__Clostridium; Unclassified_subdomains; otu_2051
OTU_97.184	Before	0.001	Root; k__Bacteria; p__Bacteroidetes; c__Bacteroidia; o__Bacteroidales; Unclassified_subdomains; otu_973
OTU_97.324	Before	0.001	Root; k__Bacteria; p__Bacteroidetes; c__Bacteroidia; o__Bacteroidales; f__Porphyromonadaceae; g__Parabacteroides; s__Parabacteroides_distasonis
OTU_97.113	Before	0.001	Root; k__Bacteria; p__Bacteroidetes; c__Bacteroidia; o__Bacteroidales; Unclassified_subdomains; otu_973
OTU_97.212	Before	0.001	Root; k__Bacteria; p__Bacteroidetes; c__Bacteroidia; o__Bacteroidales; Unclassified_subdomains; otu_973
OTU_97.156	Before	0.001	Root; k__Bacteria; p__Bacteroidetes; c__Bacteroidia; o__Bacteroidales; Unclassified_subdomains; otu_973
OTU_97.258	Before	0.001	Root; k__Bacteria; p__Bacteroidetes; c__Bacteroidia; o__Bacteroidales; Unclassified_subdomains; otu_973
OTU_97.231	Before	0.001	Root; k__Bacteria; p__Tenericutes; c__Erysipelotrichi; o__Erysipelotrichales; f__Erysipelotrichaceae; g__Allobaculum; s__Allobaculum_sp_ID4
OTU_97.199	Before	0.001	Root; k__Bacteria; p__Bacteroidetes; c__Bacteroidia; o__Bacteroidales; Unclassified_subdomains; otu_973
OTU_97.183	Before	0.001	Root; k__Bacteria; p__Bacteroidetes; c__Bacteroidia; o__Bacteroidales; Unclassified_subdomains; otu_973
OTU_97.290	Before	0.001	Root; k__Bacteria; p__Bacteroidetes; c__Bacteroidia; o__Bacteroidales; Unclassified_subdomains; otu_973
OTU_97.190	Before	0.001	Root; k__Bacteria

OTU_97.227	Before	0.001	Root; k__Bacteria
OTU_97.163	Before	0.001	Root; k__Bacteria; p__Actinobacteria; c__Actinobacteria_(class); o__Actinomycetales; f__Propionibacteriaceae; g__Propionibacterium; s__Propionibacterium_acnes
OTU_97.590	Before	0.001	Root; k__Bacteria; p__Firmicutes; c__Clostridia; o__Clostridiales; f__Catabacteriaceae; otu_1948
OTU_97.402	Before	0.001	Root; k__Bacteria; p__Bacteroidetes; c__Bacteroidia; o__Bacteroidales; Unclassified_subdomains; otu_973
OTU_97.451	Before	0.001	Root; k__Bacteria; p__TM7; c__TM7-3; o__CW040; otu_4233
OTU_97.115	Before	0.002	Root; k__Bacteria; p__Bacteroidetes; c__Bacteroidia; o__Bacteroidales; f__Prevotellaceae; g__Prevotella; Unclassified_subdomains; otu_1016
OTU_97.228	Before	0.002	Root; k__Bacteria; p__Bacteroidetes; c__Bacteroidia; o__Bacteroidales; Unclassified_subdomains; otu_973
OTU_97.399	Before	0.002	Root; k__Bacteria; p__Firmicutes; c__Clostridia; o__Clostridiales; f__Lachnospiraceae; Unclassified_subdomains; otu_2037
OTU_97.103	Before	0.002	Root; k__Bacteria; p__Bacteroidetes; c__Bacteroidia; o__Bacteroidales; Unclassified_subdomains; otu_973
OTU_97.221	Before	0.002	Root; k__Bacteria; p__Proteobacteria; c__Betaproteobacteria; o__Burkholderiales; f__Alcaligenaceae; Unclassified_subdomains; otu_2858
OTU_97.94	Before	0.002	Root; k__Bacteria; p__Cyanobacteria; c__Synechococcophycideae; o__Synechococcales; f__Synechococcaceae; g__Prochlorococcus; otu_1472
OTU_97.206	Before	0.003	Root; k__Bacteria; p__Bacteroidetes; c__Bacteroidia; o__Bacteroidales; f__Rikenellaceae; g__Alistipes; Unclassified_subdomains; otu_1035
OTU_97.600	Before	0.003	Root; k__Bacteria; p__Firmicutes; c__Clostridia; o__Clostridiales; f__Lachnospiraceae; Unclassified_subdomains; otu_2037
OTU_97.423	Before	0.003	Root; k__Bacteria; p__Firmicutes; c__Clostridia; o__Clostridiales; f__Lachnospiraceae; Unclassified_subdomains; otu_2037
OTU_97.786	Before	0.003	Root; k__Bacteria; p__Firmicutes; c__Clostridia; o__Clostridiales; f__Lachnospiraceae; g__Clostridium; Unclassified_subdomains; otu_2051

OTU_97.242	Before	0.004	Root; k__Bacteria; p__Cyanobacteria; c__Synechococcophycideae; o__Synechococcales; f__Synechococcaceae; g__Prochlorococcus; otu_1472
OTU_97.187	Before	0.004	Root; k__Bacteria; p__Bacteroidetes; c__Bacteroidia; o__Bacteroidales; Unclassified_subdomains; otu_973
OTU_97.552	Before	0.004	Root; k__Bacteria; p__Firmicutes; c__Clostridia; o__Clostridiales; f__Lachnospiraceae; Unclassified_subdomains; otu_2037
OTU_97.291	Before	0.004	Root; k__Bacteria; p__Firmicutes; c__Clostridia; o__Clostridiales; f__Ruminococcaceae; g__Ruminococcus; Unclassified_subdomains; otu_2128
OTU_97.210	Before	0.005	Root; k__Bacteria; p__Bacteroidetes; c__Bacteroidia; o__Bacteroidales; Unclassified_subdomains; otu_973
OTU_97.369	Before	0.005	Root; k__Bacteria; p__Bacteroidetes; c__Bacteroidia; o__Bacteroidales; Unclassified_subdomains; otu_973
OTU_97.598	Before	0.005	Root; k__Bacteria; p__Bacteroidetes; c__Bacteroidia; o__Bacteroidales; Unclassified_subdomains; otu_973
OTU_97.311	Before	0.005	Root; k__Bacteria; p__Firmicutes; c__Clostridia; o__Clostridiales; f__Lachnospiraceae; Unclassified_subdomains; otu_2037
OTU_97.219	Before	0.006	Root; k__Bacteria; p__Proteobacteria; c__Epsilonproteobacteria; o__Campylobacterales; f__Helicobacteraceae; g__Helicobacter; s__Helicobacter_hepaticus
OTU_97.514	Before	0.007	Root; k__Bacteria; p__Firmicutes; c__Clostridia; o__Clostridiales; f__Lachnospiraceae; Unclassified_subdomains; otu_2037
OTU_97.262	Before	0.008	Root; k__Bacteria; p__Proteobacteria; c__Gammaproteobacteria; o__Thiotrichales; f__Francisellaceae; Unclassified_subdomains; otu_3833
OTU_97.392	Before	0.008	Root; k__Bacteria; p__Bacteroidetes; c__Bacteroidia; o__Bacteroidales; f__Bacteroidaceae; g__Bacteroides
OTU_97.277	Before	0.009	Root; k__Bacteria; p__Bacteroidetes; c__Bacteroidia; o__Bacteroidales; f__Bacteroidaceae; g__Bacteroides; s__Bacteroides_acidifaciens
OTU_97.558	Before	0.01	Root; k__Bacteria; p__Proteobacteria; c__Deltaproteobacteria; o__Desulfovibrionales; f__Desulfovibrionaceae; g__Desulfovibrio; Unclassified_subdomains; otu_3126

OTU_97.506	Before	0.012	Root; k__Bacteria; p__Firmicutes; c__Clostridia; o__Clostridiales; f__Lachnospiraceae; Unclassified_subdomains; otu_2037
OTU_97.257	Before	0.014	Root; k__Bacteria; p__Deferribacteres; c__Deferribacteres_(class); o__Deferribacterales; f__Deferribacteraceae; g__Mucispirillum; s__Mucispirillum_schaedleri
OTU_97.625	Before	0.015	Root; k__Bacteria; p__Firmicutes; c__Clostridia; o__Clostridiales; f__Lachnospiraceae; Unclassified_subdomains; otu_2037
OTU_97.585	Before	0.018	Root; k__Bacteria; p__Bacteroidetes; c__Bacteroidia; o__Bacteroidales; f__Prevotellaceae; g__Prevotella; Unclassified_subdomains; otu_1016
OTU_97.1010	Before	0.018	Root; k__Bacteria; p__Firmicutes; c__Clostridia; o__Clostridiales; f__Ruminococcaceae
OTU_97.356	Before	0.022	Root; k__Bacteria; p__Firmicutes; c__Clostridia; o__Clostridiales; f__Lachnospiraceae; Unclassified_subdomains; otu_2037
OTU_97.416	Before	0.022	Root; k__Bacteria; p__Bacteroidetes; c__Bacteroidia; o__Bacteroidales; Unclassified_subdomains; otu_973
OTU_97.332	Before	0.022	Root; k__Bacteria; p__Firmicutes; c__Clostridia; o__Clostridiales; f__Lachnospiraceae; Unclassified_subdomains; otu_2037
OTU_97.45	Before	0.026	Root; k__Bacteria; p__Proteobacteria; c__Gammaproteobacteria; o__Oceanospirillales
OTU_97.866	Before	0.03	Root; k__Bacteria; p__Firmicutes; c__Clostridia; o__Clostridiales; f__Ruminococcaceae
OTU_97.466	Before	0.032	Root; k__Bacteria; p__Firmicutes; c__Bacilli; o__Lactobacillales; f__Streptococcaceae; g__Streptococcus
OTU_97.211	Before	0.033	Root; k__Bacteria
OTU_97.737	Before	0.033	Root; k__Bacteria; p__Firmicutes; c__Clostridia; o__Clostridiales; f__Lachnospiraceae; Unclassified_subdomains; otu_2037
OTU_97.919	Before	0.036	Root; k__Bacteria; p__Firmicutes; c__Clostridia; o__Clostridiales; f__Lachnospiraceae; Unclassified_subdomains; otu_2037
OTU_97.1380	Before	0.037	Root; k__Bacteria; p__Bacteroidetes; c__Bacteroidia; o__Bacteroidales; Unclassified_subdomains; otu_973
OTU_97.363	Before	0.038	Root; k__Bacteria; p__Firmicutes; c__Clostridia; o__Clostridiales; f__Lachnospiraceae; Unclassified_subdomains; otu_2037
OTU_97.10	Before	0.048	Root; k__Bacteria; p__Bacteroidetes; c__; o__; f__; Unclassified_subdomains; otu_966

OTU_97.57	During	0.001	Root; k__Bacteria; p__Proteobacteria; c__Gammaproteobacteria; o__Oceanospirillales; f__Pseudomonadaceae; g__Pseudomonas
OTU_97.350	During	0.002	Root; k__Bacteria; p__Proteobacteria; c__Gammaproteobacteria; o__Pseudomonadales; f__Moraxellaceae; g__Psychrobacter; Unclassified_subdomains; otu_3819
OTU_97.607	During	0.016	Root; k__Bacteria; p__Firmicutes; c__Bacilli; o__Bacillales; f__Bacillaceae; g__Bacillus; s__Bacillus_anthracis
OTU_97.141	During	0.024	Root; k__Bacteria; p__Proteobacteria; c__Alphaproteobacteria; o__Rhizobiales; f__Bradyrhizobiaceae
OTU_97.76	During	0.026	Root; k__Bacteria
OTU_97.1177	During	0.027	Root; k__Bacteria; p__Proteobacteria; c__Gammaproteobacteria; o__Enterobacteriales; f__Enterobacteriaceae; g__Erwinia; Unclassified_subdomains; otu_3487
OTU_97.471	During	0.043	Root; k__Bacteria; p__Proteobacteria; c__Alphaproteobacteria; o__Rickettsiales; f__Rickettsiaceae
OTU_97.136	After	0.001	Root; k__Bacteria; p__Proteobacteria; c__Alphaproteobacteria; o__Rhodobacterales; f__Rhodobacteraceae
OTU_97.93	After	0.004	Root; k__Bacteria; p__Proteobacteria; c__Alphaproteobacteria; o__Rhizobiales
OTU_97.91	After	0.005	Root; k__Bacteria; p__Verrucomicrobia; c__Verrucomicrobiae; o__Verrucomicrobiales; f__Verrucomicrobiaceae; g__Rubritalea; otu_4261
OTU_97.148	After	0.007	Root; k__Bacteria; p__Proteobacteria; c__Alphaproteobacteria; o__Rhodobacterales; f__Rhodobacteraceae
OTU_97.193	After	0.008	Root; k__Bacteria; p__Verrucomicrobia; c__Verrucomicrobiae; o__Verrucomicrobiales; f__Verrucomicrobiaceae; g__Rubritalea; otu_4261
OTU_97.41	After	0.009	Root; k__Bacteria; p__Verrucomicrobia; c__Verrucomicrobiae; o__Verrucomicrobiales; f__Verrucomicrobiaceae; g__Rubritalea; otu_4261
OTU_97.248	After	0.009	Root; k__Bacteria; p__Verrucomicrobia; c__Verrucomicrobiae; o__Verrucomicrobiales; f__Verrucomicrobiaceae; g__Rubritalea; otu_4261
OTU_97.315	After	0.01	Root; k__Bacteria; p__Proteobacteria; c__Alphaproteobacteria; o__Rhodobacterales; f__Rhodobacteraceae; g__Ruegeria; Unclassified_subdomains; otu_2655
OTU_97.7	After	0.011	Root; k__Bacteria; p__Proteobacteria; c__Gammaproteobacteria; o__Oceanospirillales
OTU_97.130	After	0.011	Root; k__Bacteria; p__Cyanobacteria; c__Synechococcophycideae; o__Pseudanabaenales;

			f__Pseudanabaenaceae; g__Halomicronema; otu_1458
OTU_97.318	After	0.014	Root; k__Bacteria
OTU_97.445	After	0.02	Root; k__Bacteria; p__Bacteroidetes; c__; o__; f__; Unclassified_subdomains; otu_966
OTU_97.308	After	0.023	Root; k__Bacteria; p__Bacteroidetes; c__Sphingobacteria; o__Sphingobacteriales; f__; Unclassified_subdomains; otu_1153
OTU_97.347	After	0.025	Root; k__Bacteria; p__Cyanobacteria; c__Chloroplast; o__Cercozoa; f__Chlorarachniophyceae; otu_1356
OTU_97.139	After	0.025	Root; k__Bacteria
OTU_97.586	After	0.025	Root; k__Bacteria; p__Proteobacteria; c__Gammaproteobacteria; o__Oceanospirillales
OTU_97.382	After	0.028	Root; k__Bacteria; p__Proteobacteria; c__Alphaproteobacteria; o__Rhizobiales
OTU_97.412	After	0.03	Root; k__Bacteria; p__Proteobacteria; c__Alphaproteobacteria; o__Rhizobiales; Unclassified_subdomains; otu_2396
OTU_97.783	After	0.032	Root; k__Bacteria; p__Proteobacteria; c__Gammaproteobacteria; o__Oceanospirillales
OTU_97.245	After	0.033	Root; k__Bacteria; p__Cyanobacteria; c__Chloroplast; o__Stramenopiles; otu_1367
OTU_97.431	After	0.033	Root; k__Bacteria; p__Proteobacteria; c__Alphaproteobacteria; o__Rhizobiales
OTU_97.317	After	0.033	Root; k__Bacteria; p__Proteobacteria; c__Alphaproteobacteria; o__Rhizobiales; f__Phyllobacteriaceae; Unclassified_subdomains; otu_2500
OTU_97.60	After	0.034	Root; k__Bacteria; p__Bacteroidetes; c__; o__; f__; Unclassified_subdomains; otu_966
OTU_97.309	After	0.034	Root; k__Bacteria; p__Bacteroidetes; c__Sphingobacteria; o__Sphingobacteriales; f__Flammeovirgaceae; g__Persicobacter; s__Persicobacter_diffluens
OTU_97.286	After	0.034	Root; k__Bacteria; p__Firmicutes; c__Clostridia; o__Clostridiales
OTU_97.988	After	0.035	Root; k__Bacteria; p__Proteobacteria; c__Gammaproteobacteria; o__Pseudomonadales; f__Moraxellaceae; g__Psychrobacter; s__Psychrobacter_celer
OTU_97.908	After	0.038	Root; k__Bacteria; p__Bacteroidetes; c__Flavobacteria; o__Flavobacteriales
OTU_97.216	After	0.038	Root; k__Bacteria; p__Proteobacteria; c__Alphaproteobacteria; o__Rhodobacterales; f__Rhodobacteraceae

OTU_97.359	After	0.045	Root; k__Bacteria; p__Cyanobacteria; c__Chloroplast
OTU_97.367	After	0.047	Root; k__Bacteria; p__Bacteroidetes; c__Flavobacteria
OTU_97.97	After	0.048	Root; k__Bacteria; p__Proteobacteria; c__Gammaproteobacteria; o__Vibrionales; f__Vibrionaceae
OTU_97.1056	After	0.049	Root; k__Bacteria; p__Proteobacteria; c__Alphaproteobacteria; o__Rhodobacterales; f__Rhodobacteraceae
OTU_97.580	After	0.05	Root; k__Bacteria; p__Proteobacteria; c__Alphaproteobacteria; o__Rhizobiales
OTU_97.59	Long After	0.001	Root; k__Bacteria; p__Proteobacteria; c__Betaproteobacteria; o__Burkholderiales; f__Oxalobacteraceae; g__Massilia; s__Massilia_timonae
OTU_97.2	Long After	0.001	Root; k__Bacteria
OTU_97.1387	Long After	0.001	Root; k__Bacteria
OTU_97.710	Long After	0.001	Root; k__Bacteria; p__Cyanobacteria; c__Chloroplast; o__; f__; g__CAB-I; otu_1354
OTU_97.64	Long After	0.001	Root; k__Bacteria; p__Proteobacteria; c__Alphaproteobacteria; o__Sphingomonadales; f__Sphingomonadaceae; g__Sphingomonas; s__Sphingomonas_yabuuchiae
OTU_97.232	Long After	0.001	Root; k__Bacteria; p__Cyanobacteria; c__Chloroplast; o__; f__; g__CAB-I; otu_1354
OTU_97.696	Long After	0.001	Root; k__Bacteria
OTU_97.304	Long After	0.001	Root; k__Bacteria; p__Actinobacteria; c__Actinobacteria_(class); o__Actinomycetales; f__Micromonosporaceae; g__Dactylosporangium; otu_553
OTU_97.77	Long After	0.001	Root; k__Bacteria; p__Proteobacteria; c__Alphaproteobacteria; o__Sphingomonadales; f__Sphingomonadaceae; g__Sphingomonas; Unclassified_subdomains; otu_2819
OTU_97.1639	Long After	0.002	Root; k__Bacteria
OTU_97.1373	Long After	0.003	Root; k__Bacteria; p__Cyanobacteria; c__Chloroplast; o__; f__; g__CAB-I; otu_1354
OTU_97.1449	Long After	0.004	Root; k__Bacteria; p__Cyanobacteria; c__Chloroplast; o__; f__; g__CAB-I; otu_1354
OTU_97.432	Long After	0.004	Root; k__Bacteria
OTU_97.1577	Long After	0.005	Root; k__Bacteria; p__Proteobacteria; c__Deltaproteobacteria; o__CTD005-82B-02; otu_3099

OTU_97.181	Long After	0.005	Root; k__Bacteria; p__Proteobacteria; c__Gammaproteobacteria; o__Enterobacteriales; f__Enterobacteriaceae; g__Erwinia; s__Erwinia_tasmaniensis
OTU_97.387	Long After	0.007	Root; k__Bacteria; p__Cyanobacteria; c__Chloroplast; o__Stramenopiles; otu_1367
OTU_97.1384	Long After	0.007	Root; k__Bacteria; p__Proteobacteria; c__Alphaproteobacteria; o__Rhodobacterales; f__Rhodobacteraceae
OTU_97.1505	Long After	0.007	Root; k__Bacteria; p__Proteobacteria; c__Betaproteobacteria; o__Burkholderiales; f__Oxalobacteraceae; g__Massilia; s__Massilia_timonae
OTU_97.1394	Long After	0.007	Root; k__Bacteria; p__Proteobacteria; c__Betaproteobacteria; o__Burkholderiales; f__Oxalobacteraceae; g__Massilia; s__Massilia_timonae
OTU_97.1186	Long After	0.008	Root; k__Bacteria; p__Proteobacteria; c__Alphaproteobacteria; o__Rhodobacterales; f__Rhodobacteraceae
OTU_97.53	Long After	0.009	Root; k__Bacteria; p__Chloroflexi; c__Anaerolineae; o__S0208; otu_1308
OTU_97.797	Long After	0.009	Root; k__Bacteria; p__Proteobacteria; c__Alphaproteobacteria; o__Sphingomonadales; f__Erythrobacteraceae; g__Erythrobacter; Unclassified_subdomains; otu_2788
OTU_97.591	Long After	0.01	Root; k__Bacteria; p__Proteobacteria; c__Gammaproteobacteria; o__Alteromonadales; f__Pseudoalteromonadaceae; g__Pseudoalteromonas
OTU_97.72	Long After	0.012	Root; k__Bacteria; p__Proteobacteria; c__Alphaproteobacteria
OTU_97.1638	Long After	0.012	Root; k__Bacteria; p__Proteobacteria; c__Alphaproteobacteria; o__Rhodobacterales; f__Rhodobacteraceae; g__Ruegeria; Unclassified_subdomains; otu_2655
OTU_97.1099	Long After	0.016	Root; k__Bacteria
OTU_97.98	Long After	0.017	Root; k__Bacteria
OTU_97.960	Long After	0.017	Root; k__Bacteria
OTU_97.743	Long After	0.019	Root; k__Bacteria; p__Chloroflexi; c__Anaerolineae; o__S0208; otu_1308
OTU_97.443	Long After	0.022	Root; k__Bacteria
OTU_97.1050	Long After	0.023	Root; k__Bacteria
OTU_97.1822	Long After	0.026	Root; k__Bacteria

OTU_97.1389	Long After	0.029	Root; k__Bacteria; p__Cyanobacteria; c__Chloroplast; o__; f__; g__CAB-I; otu_1354
OTU_97.1758	Long After	0.033	Root; k__Bacteria
OTU_97.884	Long After	0.034	Root; k__Bacteria; p__Cyanobacteria; c__Synechococcophycideae; o__Pseudanabaenales; f__Pseudanabaenaceae; g__Halomicronema; otu_1458
OTU_97.1190	Long After	0.035	Root; k__Bacteria; p__Proteobacteria; c__Gammaproteobacteria; o__Alteromonadales; f__Colwelliaceae
OTU_97.2180	Long After	0.039	Root; k__Bacteria
OTU_97.209	Long After	0.044	Root; k__Bacteria
OTU_97.934	Long After	0.044	Root; k__Bacteria; p__Proteobacteria; c__Betaproteobacteria; o__Burkholderiales; f__Oxalobacteraceae; g__Massilia; s__Massilia_timonae
OTU_97.1997	Long After	0.044	Root; k__Bacteria; p__Proteobacteria; c__Gammaproteobacteria; o__Legionellales
OTU_97.955	Long After	0.045	Root; k__Bacteria; p__Actinobacteria; c__Actinobacteria_(class); o__Actinomycetales; f__Dermacoccaceae; g__Dermacoccus; otu_376
OTU_97.2129	Long After	0.047	Root; k__Bacteria; p__Bacteroidetes; c__Sphingobacteria; o__Sphingobacteriales; f__Flammeovirgaceae; Unclassified_subdomains; otu_1173
OTU_97.606	Long After	0.047	Root; k__Bacteria; p__Bacteroidetes; c__Sphingobacteria; o__Sphingobacteriales; f__Flammeovirgaceae; Unclassified_subdomains; otu_1173

Table S1.4: Results of indicspecies analysis for *O. faveolata,* bleached vs. unbleached

OTU	**Group Association**	**p value**	**Taxonomy**
OTU_97.197	Bleached	0.002	Root; k__Bacteria
OTU_97.536	Bleached	0.009	Root; k__Bacteria; p__Proteobacteria; c__Alphaproteobacteria
OTU_97.48	Bleached	0.01	Root; k__Bacteria; p__Proteobacteria; c__Alphaproteobacteria; o__Rickettsiales; Unclassified_subdomains; otu_2747
OTU_97.143	Bleached	0.011	Root; k__Bacteria; p__Bacteroidetes; c__Flavobacteria
OTU_97.593	Bleached	0.011	Root; k__Bacteria; p__Bacteroidetes
OTU_97.85	Bleached	0.017	Root; k__Bacteria; p__Bacteroidetes; c__; o__; f__; g__Candidatus_Cardinium

OTU_97.885	Bleached	0.025	Root; k__Bacteria; p__Proteobacteria; c__Alphaproteobacteria
OTU_97.189	Bleached	0.032	Root; k__Bacteria; p__Bacteroidetes; c__Flavobacteria; o__Flavobacteriales; f__Flavobacteriaceae; Unclassified_subdomains; otu_1051
OTU_97.297	Bleached	0.037	Root; k__Bacteria; p__Bacteroidetes; c__Flavobacteria; o__Flavobacteriales; f__Flavobacteriaceae
OTU_97.525	Bleached	0.038	Root; k__Bacteria
OTU_97.1136	Bleached	0.038	Root; k__Bacteria; p__Proteobacteria; c__Alphaproteobacteria
OTU_97.1666	Healthy	0.025	Root; k__Bacteria; p__Bacteroidetes; c__; o__; f__; Unclassified_subdomains; otu_966
OTU_97.2133	Healthy	0.043	Root; k__Bacteria; p__Bacteroidetes; c__; o__; f__

Table S1.5. Results of negative binomial generalized linear models in *G. ventalina* and *O. faveolata.* Multiple models are listed when the delta AIC is less than two as these are all plausible models for the data.

Focal Taxon	***G. ventalina*: Best fit model**	**FDR adjusted p-values** (α=0.05)	***O. faveolata*: Best fit model**	**FDR adjusted p-values** (α=0.05)
Bacteroidetes (Phylum)	Null		Null	
Acidobacter (Phylum)	Null	Recovery 1 vs. Recovery 2: 0.0262	Not run (standard errors in zero-inflated model too large)	
Cyanobacteria (Phylum)	Null		Null	
Gammaproteobacteria (Class)	Null		Null	
Alphaproteobacteria (Class)	Null		Null	
Clostridia (Class)	Timing	Before vs. During: 1.85e-05	Timing	During vs. Recovery 2: 0.00136
Oceanospirillales (Order)	Timing		Null	
Rhodobacteraceae (Family)	Null		Null	
Rickettsiaceae (Family)	Null		Not run (standard errors in zero-	

			inflated model too large)	
Pseudomonadaceae (Family within Oceanospirillales)	Timing	During vs. Recovery 1: 0.00850 Recovery 1 vs. Recovery 2: 0.0102	Null	

Figure S1.1: *O. faveolata* (in red) and *G. ventalina* (in blue) do not differ in alpha diversity as calculated by a Shannon diversity index (QIIME). Error bars are standard deviation.

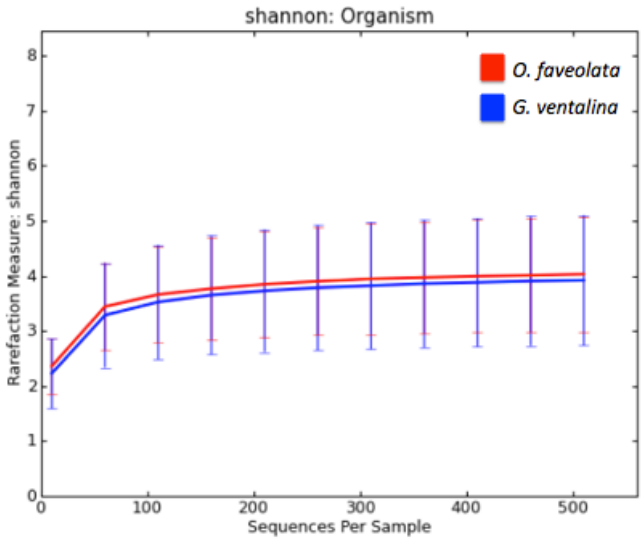

Figure S1.2: *G. ventalina* colonies before the warming event (in blue) have significantly higher alpha diversity as calculated by a Shannon diversity index (QIIME) relative to the alpha diversity among the same colonies sampled in subsequent sampling times. Error bars are standard deviation.

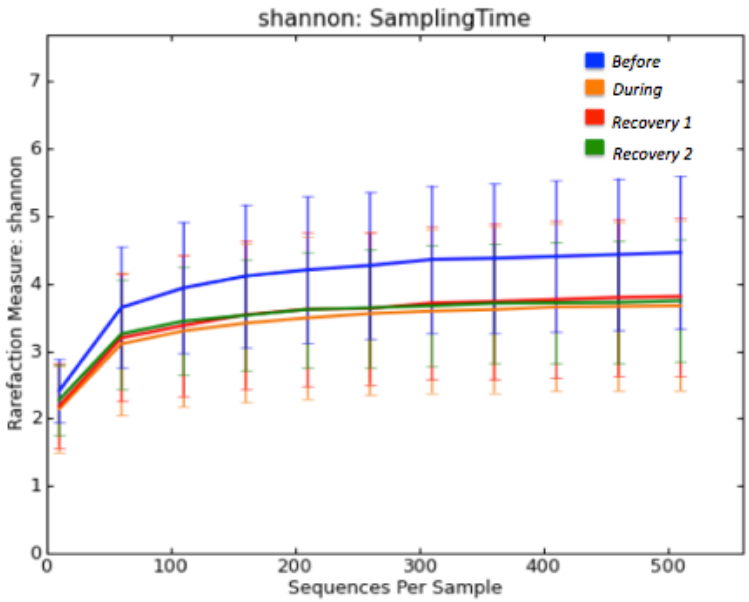

Figure S1.3: *O. faveolata* colonies during the warming event (in blue), in Recovery 1 (red) and Recovery 2 (orange). The only significant difference is that alpha diversity, as calculated by a Shannon diversity index (QIIME), is higher in Recovery 2 than in Recovery 1. Error bars are standard deviation.

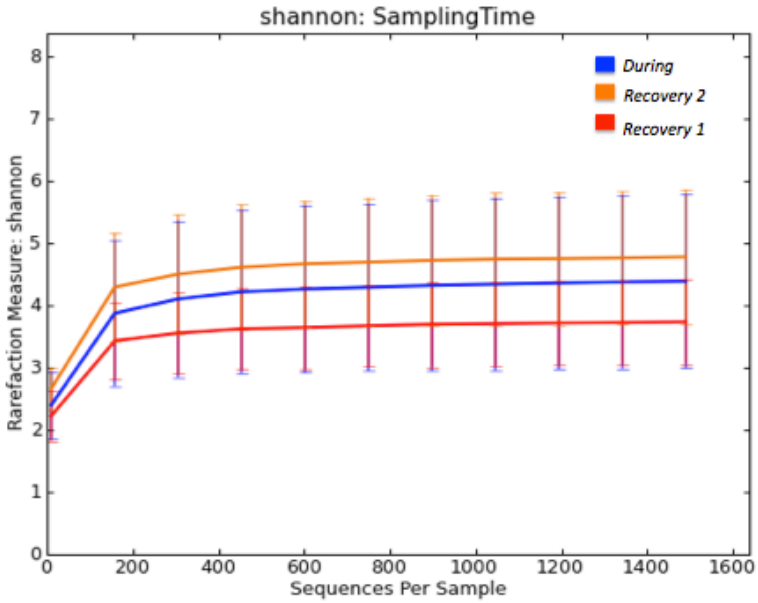

Figure S1.4: Taxa summary of *O. faveolata* phyla by sampling time, left to right: during, Recovery 1 or Recovery 2

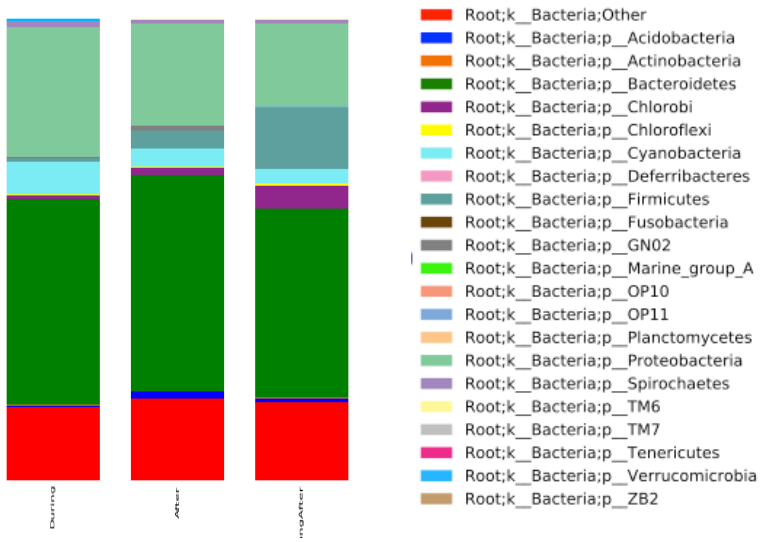

CHAPTER 2

Table S2.1: GPS Coordinates of Sites in La Parguera, Puerto Rico

Reef-site	**Latitude**	**Longitude**	**Temperature Logger**
Turrumotico	17° 55.743'	66° 58.487"	iButton
Turrumote	17° 56.097'	67° 01.130"	HOBO
Laurel Patch	17° 56.537'	67° 04.057'	iButton
Media Luna	17° 56.096'	67° 02.911'	HOBO
Pelotas	17° 57.446"	67° 04.183'	HOBO
Caballo Blanco	17° 57.831'	67° 02.940'	iButton
Enrique	17° 57.294'	67° 02.608'	HOBO
Corral Channel	17° 56.959'	66° 59.938"	iButton
Fosfo Bay	17° 57.544'	67° 00.826'	iButton
Mario reef	17° 57.170'	67° 03 387'	iButton

Figure S2.1: Map of survey sites near La Parguera, PR with inset map of Puerto Rico

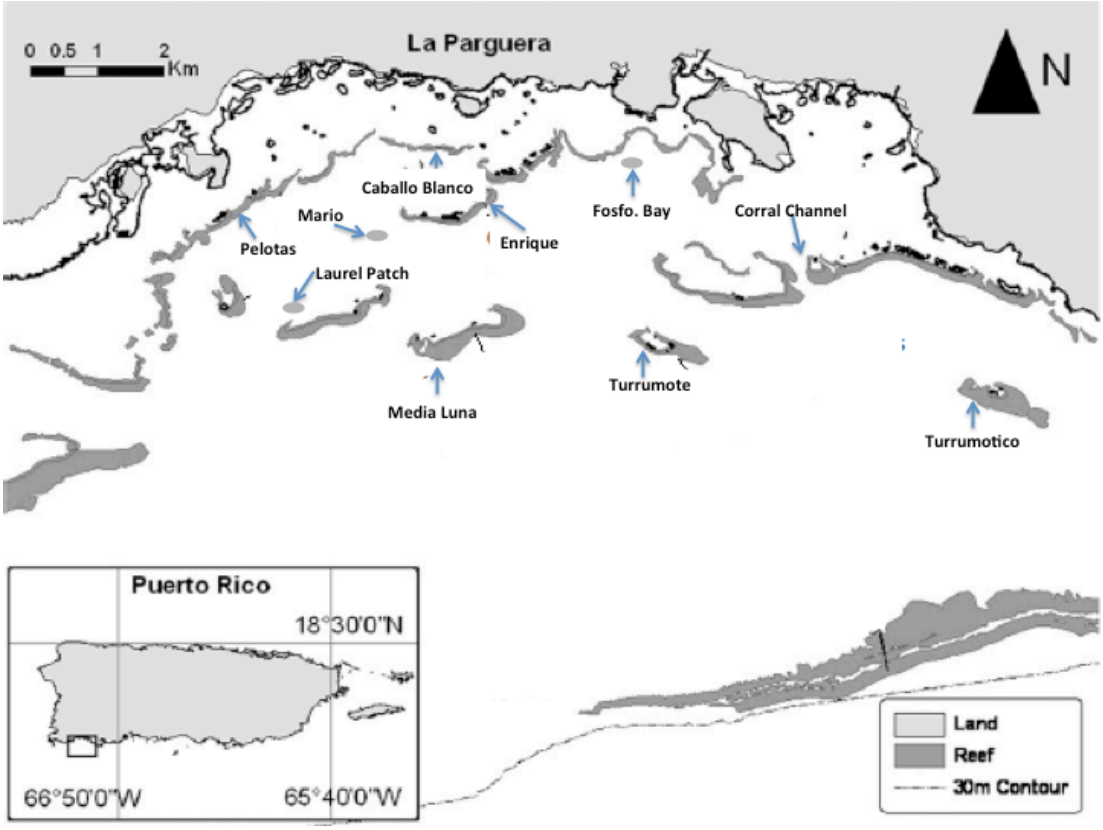

Table S2.2: AIC values for labyrinthulid prevalence models (AIC Weight > 0) with best model highlighted

Model	Degrees of freedom	Delta AIC	AIC Weight
Depth	3	0	0.28
Depth + Temperature	4	0.5	0.22
Depth + Temperature + Density	5	0.53	0.22
Depth + Temperature + Size	5	2.19	0.09
Depth + Temperature + Size + Density	6	2.24	0.09
Depth + Temperature + Size + Coral cover	6	4.18	0.04
Depth + Temperature + Size + Density + Copepod	7	4.2	0.03
Depth + Temperature + Size + Coral cover + Copepod	7	6.16	0.01
Null	2	6.82	0.01

Table S2.3: Summary of the best model of labyrinthulid prevalence (GLMM)

	Estimate	Std. error	z value	Pr(>|z|)	95% Confidence interval	Odds Ratio
(Intercept)	-3.60	0.975	-3.69	0.00022*	(-6.47, -2.06)	0.0273
Depth	5.37	1.79	3.00	0.0027*	(2.35,10.1)	214

Table S2.4: AIC values for copepod prevalence with best model highlighted

Model	Degrees of freedom	Delta AIC	AIC Weight
Size^2	4	0	0.23
Size^2+ Density	5	0.57	0.17
Size^2+ Labyrinthulid	5	1.98	0.09
Size + Density	5	2.14	0.08
Size^2+ Density + Temperature	6	2.29	0.07
Size^2+ Depth + Coral cover	6	3.03	0.05
Size*Density + Depth	6	3.97	0.03
Size^2+ Temperature + Density + Labyrinthulid	7	4.25	0.03
Size*Temperature	5	4.51	0.02
Null model	2	4.69	0.02

Table S2.5: Summary of the best-fit model of copepod prevalence (GLMM)

	Estimate	Std. Error	z value	Pr(>|z|)	95% Confidence interval	Odds Ratio
(Intercept)	0.111	0.332	0.334	0.74	(-0.526, 0.792)	1.12
Size	2.84	1.09	2.61	0.0091*	(0.827, 5.13)	17.1
Size^2	-2.25	1.12	-2.01	0.044*	(-4.89, -0.539)	0.105

Table S2.6: (a) AIC table of copepod prevalence models (AIC weight > 0) with best model highlighted (b) and summary of the best-fit model of copepod prevalence with the two largest sea fans omitted (GLMM)

(a)

	Degrees of Freedom	Delta AIC	AIC Weight
Size*Depth + Labyrinthulid	6	0	0.23
Size*Depth + Density + Labyrinthulid	7	0.15	0.22
Size*Temperature	5	1.08	0.14

Size*Coral cover + Labyrinthulid	6	1.22	0.13
Size*Temperature + Density + Labyrinthulid	7	1.83	0.09
Size	3	3.2	0.05
Density*Labyrinthulid + Size	6	3.66	0.04
Size + Density + Labyrinthulid	5	4.24	0.03
Size*Density + Labyrinthulid	6	5.57	0.01
Coral cover*Labyrinthulid + Size	6	5.58	0.01
Coral cover^2 + Size + Labyrinthulid	6	6.8	0.01
Depth*Density + Size + Labyrinthulid	7	6.99	0.01
Depth*Labyrinthulid + Size	6	7.08	0.01
Depth^2 + Density + Size + Labyrinthulid	7	7.35	0.01

(b)

	Estimate	**Std. error**	**z value**	**Pr (>|z|)**	**95% Confidence interval**	**Odds Ratio**
(Intercept)	0.0518	0.363	0.142	0.89	(-0.659, 0.788)	1.05
Size	3.11	1.03	3.02	0.0026	(1.31, 5.42)	22.4
Depth	0.134	0.686	0.195	0.846	(-1.20, 1.53)	1.14
Labyrinthulid	-1.54	0.978	-1.58	0.115	(-3.76, 0.196)	0.214
Size: Depth	4.22	1.73	2.44	0.015	(1.11, 7.98)	67.8

Table S2.7: AIC values for MFPS prevalence models with best model highlighted

Model	**Degrees of freedom**	**Delta AIC**	**AIC Weight**
Size^2+ Depth	6	0	0.6
Size^2+ Depth + Temperature	7	1.57	0.28
Size^2+ Depth + Temperature + Coral cover	8	3.23	0.12
Null	3	105.12	0

Table S2.8: Summary of best model of MFPS Prevalence (GLMM)

	Estimate	**Std. error**	**z value**	**Pr (>|z|)**	**95% Confidence interval**	**Odds Ratio**
(Intercept)	-0.582	0.139	-4.17	3.0 E-05	(-0.884, -0.290)	0.559
Size	2.10	0.231	9.10	<2.0 E-16	(1.65, 2.56)	8.14
Size^2	-0.826	0.170	-4.85	1.3 E-06	(-1.18, -0.519)	0.438
Depth	-0.858	0.260	-3.29	0.00099	(-1.42, -0.322)	0.424

Table S2.9: AICc values for MFPS severity models (censReg) with best model highlighted: Overdispersion requires a Quasi-Poisson correction. We log transformed the data for use in censReg because exploratory models using lmer established that log transforming the MFPS severity data yields the appropriate standard errors that would result from the underlying mechanics of the Quasi-Poisson correction.

Model	Degrees of freedom	Delta AICc	AICc weight
Size^2+ Depth	6	0	0.46
Size^2+ Coral cover	6	1.21	0.25
Size^2	5	2.36	0.14
Size^2+ Temperature	6	3.35	0.09
Size^2+ Density	6	4.32	0.05

Table S2.10: Summary of the best model of MFPS severity (censReg) with Wald 95% Confidence intervals

	Estimate	Std. error	t value	Pr (>t)	95% Confidence interval
(Intercept)	1.94	2.254	0.863	0.39	(-2.47, 6.36)
Size	0.527	0.147	3.59	3.3 E-04	(0.239,0.815)
Size^2	-0.047	0.047	-1.02	0.31	(-0.139, 0.0442)
Depth	-0.059	0.215	-0.276	0.78	(-0.481, 0.363)
logSigmaMu	-1.603	0.489	-3.28	1.0 E-03	(-2.56, -0.645)
logSigmaNu	-0.012	0.063	-0.186	0.85	(-0.135, 0.111)

Table S2.11: Summary of the prediction of copepod infection by MFPS status

	Estimate	Std. Error	z value	Pr(>|z|)	95% Confidence interval	Odds Ratio
(Intercept)	-3.30	1.02	-3.24	0.0012	(-6.18, -1.75)	0.037
MFPS Status	4.39	1.10	4.01	6.20 E-05	(2.62, 7.37)	81.0

Table S2.12: AIC values for models of amoebocyte density with best model highlighted.

	Degrees of Freedom	Delta_AIC	AIC Weight
Infection status + depth + coral cover	**10**	**1.77**	**0.23**
Null	**5**	**11.72**	**0**

Table S2.13: Summary of the best model of amoebocyte density, Infection status+ coral cover + depth. Effects for which the 95% confidence interval (method = "Wald") does not include 0 are significant.

	Estimate	Std. error	t value	95% Confidence interval
(Intercept)	4.28	0.103	41.7	(4.08, 4.48) *
Infection status: Copepod	-0.197	0.124	-1.58	(-0.440, 0.0467)
Infection status: Laby	-0.662	0.266	-2.49	(-1.18, -0.140) *
Infection status: Co-infection	-0.994	0.255	-3.9	(-1.49, -0.494) *
Depth	0.414	0.191	2.16	(0.0389, 0.789) *
Coral cover	-0.370	0.152	-2.43	(-0.667, -0.0720) *

Table S2.14: Pairwise comparisons with FDR correction for infection status in the best model of amoebocyte density, Infection status + coral cover + depth.

	Estimate	Std. error	z value	Pr(>|z|)	95% Confidence interval
Copepod vs. Neither	-0.197	0.124	-1.58	0.14	(-0.511, 0.118)
Laby vs. Neither	-0.662	0.266	-2.49	0.026	(-1.34, 0.0126)
Co-infected vs. Neither	-0.994	0.255	-3.90	0.00058	(-1.64, -0.348)
Laby vs. Copepod	-0.465	0.267	-1.74	0.12	(-1.14, 0.212)
Co-infected vs. Copepod	-0.797	0.263	-3.03	0.0074	(-1.46, -0.130)
Co-infected vs. Laby	-0.332	0.314	-1.06	0.29	(-1.13, 0.463)

Table S2.15: Summary of MFPS status as a predictor of amoebocyte density in a subset of sea fans without labyrinthulid infections. Effects for which the 95% confidence interval (method = "Wald") does not include 0 are significant.

	Estimate	Std. error	t value	95% Confidence interval
(Intercept)	4.08	0.112	36.3	(3.86, 4.30)
Healthy vs. Diseased	0.219	0.122	1.79	(-0.0205, 0.460)
Asymptomatic vs. Diseased	-0.0947	0.0701	-1.35	(-0.232, 0.0426)

Table S2.16: Pairwise comparisons with FDR correction for MFPS status as a predictor of amoebocyte density in a subset of sea fans without labyrinthulid infections.

	Estimate	Std. error	z value	Pr(>|z|)	95% Confidence interval
Healthy vs. Diseased	0.219	0.122	1.79	0.11	(-0.0649, 0.503)

Asymptomatic vs. Diseased	-0.0947	0.0701	-1.35	0.18	(-0.257, 0.068)
Asymptomatic vs. Healthy	-0.314	0.115	-2.72	0.020*	(-0.582, -0.0460)

CHAPTER 3

Table S3.1: Nanodrop quality and quantity data for all samples

Sample	**Timepoint of nanodrop**	**Concentration (ng/uL)**	**260/280**	**260/230**
A10L	pre DNAse	1696.5	2.04	2.55
	post DNAse	321.1	2.03	2.43
A9L	pre DNAse	1465.1	2.08	2.25
	post DNAse	302.3	2.27	2.11
N6L	pre DNAse	2148.1	2.07	2.44
	post DNAse	364.4	2.05	2.26
M6E	pre DNAse	3655.1	2.12	2.36
	post DNAse	341.1	2.03	2.52
M9E	pre DNAse	1744	2.13	2.55
	post DNAse	494.4	2.07	2.49
N2L	pre DNAse	2623.3	2.11	2.37
	post DNAse	369.3	2.05	2.4
M2E	pre DNAse	2092.7	2.07	2.53
	post DNAse	370.4	2.08	2.13
A1E	pre DNAse	2312.1	2.11	2.52
	post DNAse	379.2	2.22	2.13
MA6E	pre DNAse	1520.7	2.07	1.88
	post DNAse	395.5	2.12	1.6
MA1E	pre DNAse	2668	2.08	2.45
	post DNAse	343.3	2.16	2.2
M2L	pre DNAse	1112.8	2.04	2.49
	post DNAse	395.6	2.23	2.13
N10L	pre DNAse	2489.7	2.1	2.36
	post DNAse	367.8	2.19	2
A9E	pre DNAse	1220	N/A	N/A
	post DNAse	932.9	2.03	1.89
N9L	pre DNAse	1280	N/A	N/A

	post DNAse	1103.6	2.03	2.25
A2L	pre DNAse	1140	N/A	N/A
	post DNAse	973.2	2.02	2.22
A1L	pre DNAse	560	N/A	N/A
	post DNAse	564.9	2.14	1.94
N10E	pre DNAse	680	N/A	N/A
	post DNAse	728.9	1.97	2.14
MA2E	pre DNAse	886	N/A	N/A
	post DNAse	737.1	1.98	2.06
MA9L	pre DNAse	3209.3	2.09	2.36
	post DNAse	356.5		
MA10L	pre DNAse	3145.2	2.08	2.28
	post DNAse	337		
MA6L	pre DNAse	2308.3	2.12	1.74
	post DNAse	374.1		
M6L	pre DNAse	3306.4	2.07	2.43
	post DNAse	335		
M9L	pre DNAse	1726.6	2.08	2.33
	post DNAse	346.3		
M10L	pre DNAse	1783.8	2.09	2.49
	post DNAse	396.9		
N9E	pre DNAse	1067	2.06	2.51
	post DNAse	405	2.01	2.26
N6E	pre DNAse	1926.4	2.1	2.46
	post DNAse	360.9	2.05	2.24
M1L	pre DNAse	2370.4	2.13	2.32
	post DNAse	343	1.99	2.19
MA1L	pre DNAse	3112.8	2.08	2.2
	post DNAse	403.5	2.01	2.03
A6E	pre DNAse	2584.7	2.09	2.29
	post DNAse	353.4	2.15	1.99
A10E	pre DNAse	2212.9	2.08	2.34
	post DNAse	370.1	2.08	1.93
N2E	pre DNAse	3810.7	2.07	2.36
	post DNAse	314.2	2.06	2.13
MA10E	pre DNAse	2740.9	2.09	2.45
	post DNAse	327	2.11	2.09
A2E	pre DNAse	2722.8	2.07	2.39

	post DNAse	366	1.96	2.06
MA9E	pre DNAse	3185.4	2.08	2.34
	post DNAse	348.9	2.12	2.09
N1E	pre DNAse	2694.7	2.09	2.39
	post DNAse	393.3	2.14	2.1
M1E	pre DNAse	3441.5	2.09	2.33
	post DNAse	408	2.17	2.19
A6L	pre DNAse	3680.7	2.08	2.28
	post DNAse	358.5	2.08	1.99
N1L	pre DNAse	2493.7	2.17	2.37
	post DNAse	357.6	2.15	1.99
M10E	pre DNAse	3686.8	2.1	2.27
	post DNAse	511.7	2.12	1.96
MA2L	pre DNAse	3758.4	2.08	2.42
	post DNAse	415.2	2.02	1.98
MA4E	pre DNAse	3291.4	2.08	2.4
	post DNAse	375.9	2.1	2.14
A3L	pre DNAse	3631.5	2.09	2.34
	post DNAse	359.8	2.18	2.13
M7L	pre DNAse	2382.7	2.11	2.49
	post DNAse	350.1	2.13	2.14
M8L	pre DNAse	1765.9	2.1	2.56
	post DNAse	371.7	2.11	2.34
M5E	pre DNAse	2208.9	2.08	2.51
	post DNAse	410.5	2.14	2.21
A4E	pre DNAse	2834.3	2.11	2.47
	post DNAse	393.2	2.09	2.16
N8L	pre DNAse	2186	2.13	2.45
	post DNAse	385.3	2.11	2.14
A5L	pre DNAse	2676.5	2.09	2.44
	post DNAse	401.9	2.02	2.16
MA8L	pre DNAse	2013.1	2.13	2.41
	post DNAse	378	2.01	2.03
MA8E	pre DNAse	1617.7	2.17	2.41
	post DNAse	379.5	1.97	2.07
M4E	pre DNAse	1828.5	2.15	2.46
	post DNAse	374.8	2.05	2.28
N4E	pre DNAse	2830.8	2.13	2.22

	post DNAse	371.4	2.03	1.94
A8L	pre DNAse	2314.7	2.15	2.46
	post DNAse	340.5	2.13	2.24
MA5L	pre DNAse	2239.8	2.15	2.35
	post DNAse	405	2.11	2.14
MA7L	pre DNAse	2102.1	2.17	2.45
	post DNAse	335.6	2.24	2.29
A8E	pre DNAse	2015.1	2.17	2.45
	post DNAse	404	2.01	2.29
M3E	pre DNAse	2203.1	2.16	2.38
	post DNAse	365.8	2.11	2.15
MA5E	pre DNAse	2777.2	2.16	2.47
	post DNAse	374.5	2.04	2.14
M3L	pre DNAse	2988.1	2.09	2.45
	post DNAse	308.9	2.07	2.02
M5L	pre DNAse	2751.2	2.09	2.37
	post DNAse	382.6	2.14	2
A7L	pre DNAse	3005.6	2.11	2.39
	post DNAse	337.3	1.95	2.04
A7E	pre DNAse	2740	2.1	2.49
	post DNAse	323.3	2.07	2.14
M8E	pre DNAse	1843.8	2.1	2.46
	post DNAse	357.6	2	2.13
MA3E	pre DNAse	2161.3	2.12	2.47
	post DNAse	306.5	2.13	2.09
N3L	pre DNAse	2493.6	2.12	2.46
	post DNAse	335	2.12	2.08
MA4L	pre DNAse	1913.8	2.11	2.5
	post DNAse	328.8	2.15	2.09
N7L	pre DNAse	2152.8	2.08	2.4
	post DNAse	363.4	2.05	2.2
N3E	pre DNAse	2404.1	2.11	2.35
	post DNAse	362.3	2.13	2.06
MA7E	pre DNAse	2689.3	2.1	2.24
	post DNAse	373.4	2.02	2.04
M7E	pre DNAse	2240.1	2.11	2.25
	post DNAse	337.1	2.09	1.91
N8E	pre DNAse	1095.4	2.14	2.44

	post DNAse	356.3	2.05	2.24
N7E	pre DNAse	1812.6	2.1	2.43
	post DNAse	364.8	2.17	2.26
A5E	pre DNAse	3025.4	2.08	2.43
	post DNAse	396	2.1	2.3
M4L	pre DNAse	2391.9	2.09	2.41
	post DNAse	321.8	2.08	2.11
A4L	pre DNAse	2814.4	2.1	2.33
	post DNAse	362.2	2.03	2.25
MA3L	pre DNAse	2638.1	2.09	2.27
	post DNAse	388.6	2.12	2.21
N4L	pre DNAse	3368.6	2.06	2.26
	post DNAse	398.3	2.03	1.95
N5L	pre DNAse	1846.9	2.06	2.04
	post DNAse	407.7	2.1	1.82
N5E	pre DNAse	1196.6	2.03	2.39
	post DNAse	392.9	2.07	2.15
A3E	pre DNAse	1547.5	2.06	2.35
	post DNAse	368.2	2.12	1.86

Table S3.2: Primers for candidate immune genes

Name	**Direction**	**Sequence**	**Length**
EF1 *Elongation Factor 1*	Forward	ACCGCTGCTAGTTTGGATGT	20
	Reverse	TGATGAAACCGACATGGCTA	20
T5A *Tachylectin 5A*	Forward	ATTTCGGTTTTCCTCAACGA	20
	Reverse	CCTGGTGGTATGCTGCTTG	19
MMP *Matrix metalloproteinase*	Forward	ACCGTATTTCTGGACGTTGG	20
	Reverse	CGGTTTTTCCATCTCGTCTT	20
IκB *NF-κB Inhibitor cactus*	Forward	TCGAAGCATTGAGGTGTTGGA	21
	Reverse	GACGTGCGATATTTGCTGGC	20

Table S3.3: Efficiencies of genes from PCR Miner, averaged across Miner runs

Gene	**Efficiency**
EF1	0.882

T5A	0.803
IκB	0.860
MMP	0.853

Table S3.4: GPS coordinates of sites in La Parguera and Guánica, Puerto Rico with the abbreviation, temperature logger type and copper concentration (Pait et al. 2007).

Reef site name and #	**Latitude**	**Longitude**	**Temperature Logger**	**Copper sediment concentration range**
Turrumotico (#1) "TC"	17° 55.743'	66° 58.487"	Use Turrumote	0.0-0.9 µg/g
Turrumote (#2) "TM"	17° 56.097'	67° 01.130"	HOBO	1.0-1.9 µg/g (Indicator Kriging, Pait et al. 2007)
Laurel Patch (#3) "L"	17° 56.537'	67° 04.057'	Use Media Luna	0.0-0.9 µg/g
Media Luna (#4) "ML"	17° 56.096'	67° 02.911'	HOBO	2.0-4.1 µg/g
Pelotas (#5) "P"	17° 57.446"	67° 04.183'	HOBO	2.0-4.1 µg/g
Caballo Blanco (#6) "CB"	17° 57.831'	67° 02.940'	iButton	2.0-4.1 µg/g
Enrique (#7) "E"	17° 57.294'	67° 02.608'	HOBO	4.2-80.6 µg/g
Corral Channel (#8) "CH"	17° 56.959'	66° 59.938"	iButton	4.2-80.6 µg/g
Fosfo Bay (#9) "F"	17° 57.544'	67° 00.826'	Use Channel	4.2-80.6 µg/g
Mario reef (#10) "M"	17° 57.170'	67° 03 387'	HOBO	4.2-80.6 µg/g
Buoy (#11) "B"	17° 53.291"	66° 59.884'	HOBO	0.0-0.9 µg/g (Indicator Kriging, Pait et al. 2007)
Romero (#12) "R"	17° 56.830'	66° 59.431'	iButton	4.2-80.6 µg/g (Indicator Kriging, Pait et al. 2007)
San Cristobal (#13) "SC"	17° 56.497'	67° 04.497'	Use Pelotas	1.0-1.9 µg/g (Indicator

				Kriging, Pait et al. 2007)
Guánica 1 (#14) "G1"	17° 56.862'	66° 54.087'	iButton	1.0-1.9 µg/g (Indicator Kriging, Pait et al. 2007)
Guánica 2 (#15) "G2"	17° 56.529'	66° 54.855'	Use Guánica 1	1.0-1.9 µg/g

Fig. S3.1: Map of survey sites in The Natural Reserve of La Parguera and in Guánica, on the southwest coast of Puerto Rico.

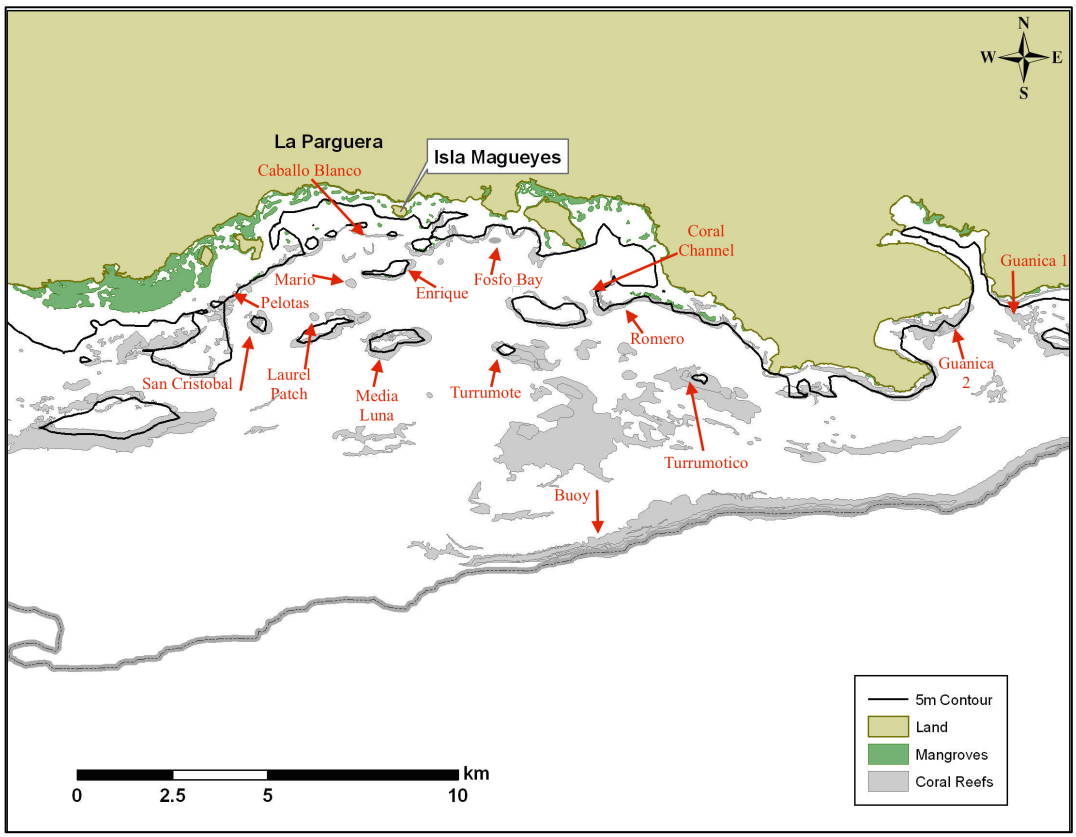

Table S3.5: Best fit random effects structures for candidate genes

Gene	Random slope	Random intercept
T5A	Time	Colony
IκB	ParasiteYN	Colony
MMP	None	Colony

Table S3.6: AIC Table of models for amoebocyte density in the laboratory experiment (random effects = 1|colony:sample) with the best model highlighted. The model with copepod alone is better than the null by the LRT (Chi Sq. = 3.99, P= 0.0457).

Model	Degrees of freedom (K)	Delta AIC	AIC Weight

Copepod	5	0	0.21
Copepod + Aspergillus	6	1.24	0.12
Parasite_single	6	1.74	0.09
Parasite	5	1.91	0.08
Copepod + time	6	1.95	0.08
Null	4	1.99	0.08
Copepod * Aspergillus	7	3.08	0.05
Copepod + Aspergillus + time	7	3.18	0.04
Aspergillus	5	3.21	0.04
Parasite_single + time	7	3.68	0.03
Parasite + time	6	3.84	0.03
Copepod * time	7	3.93	0.03
Copepod+Aspergillus*time	8	4.09	0.03
Copepod * Aspergillus + time	8	5.03	0.02
Copepod * time + Aspergillus	8	5.15	0.02
Aspergillus + time	6	5.15	0.02
Parasite *time	7	5.65	0.01
Aspergillus * time	7	6.22	0.01
Parasite_single *time	9	6.75	0.01
Copepod*Aspergillus*time	11	9.75	0

Table S3.7: The best model of laboratory amoebocyte density includes the copepod as a predictor.

Random effects:						
	Groups	**Name**	**Variance**	**Standard deviation**		
	sample	Intercept	0.113	0.336		
	colony	Intercept	0.120	0.346		
	Residual	0.424	0.651			
Fixed effects:						
	Estimate	**Standard Error**	**Degrees of freedom**	**t value**	**Pr(>|t|)**	**95% CI**
Intercept	4.54	0.127	8.08	35.9	3.40E-10	4.29-4.79
Copepod	0.105	0.0525	64.8	2.01	0.049	0.00242-0.208

Fig. S3.2: Amoebocyte density is best predicted by copepod infection across all 9 colonies included in the analyses.

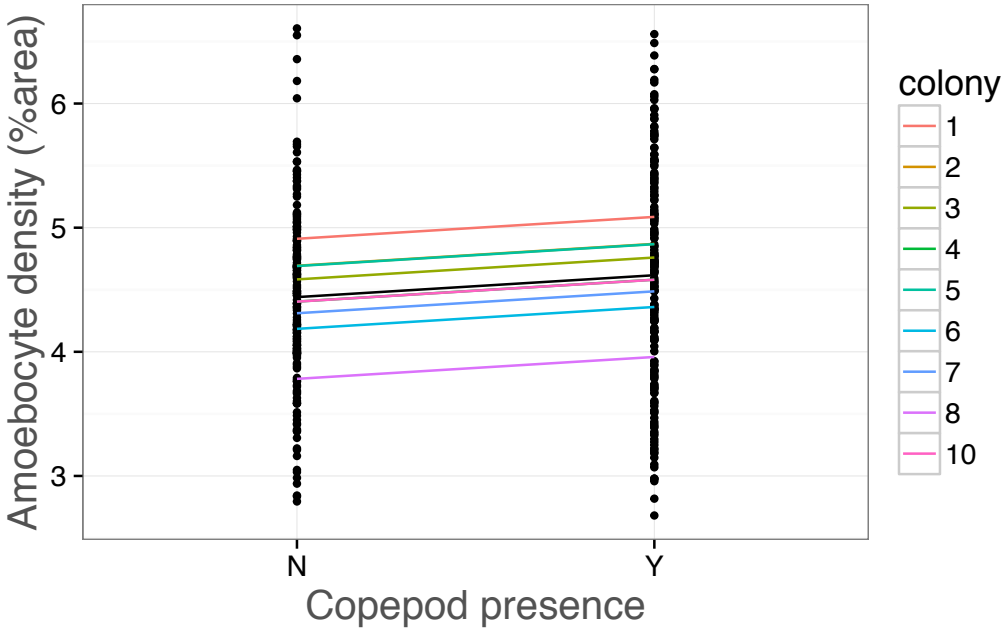

Table S3.8: None of the infection terms, time or interactions predicted EF1 expression for any of the subsets (NS = not significant; DF = degrees of freedom; LRT = likelihood ratio test). Models include colony as a random intercept. No random slopes were supported by model comparison.

EF1 (T5A samples)			**EF1 (IκB samples)**			**EF1 (MMP samples)**		
Model	**DF**	**Delta AIC**	**Model**	**DF**	**Delta AIC**	**Model**	**DF**	**Delta AIC**
Parasite*time	6	0	Parasite*time	6	0	Aspergillus*time	6	0
Null	3	2.01	Parasite_single*time	8	0.79	Aspergillus*time+copepod	7	1.5
Aspergillus*time	6	2.4	Aspergillus*time	6	3.05	Null	3	1.7
Copepod	4	2.4	Copepod*Aspergillus*time	10	4.61	Parasite*time	6	2.33
Parasite	4	2.6	Aspergillus*time+copepod	7	5.01	Parasite	4	3.07
Aspergillus*time+copepod	7	2.63	Copepod*time	6	5.59	Copepod	4	3.26
Parasite_single*time	8	3.58	Parasite+time	5	6.25	Aspergillus	4	3.55

Aspergillus	4	4.01	Copepod+time	5	7.2	Parasite+time	5	4.09
Copepod+time	5	4.06	Aspergillus+time	5	7.21	Copepod+time	5	4.28
Parasite+time	5	4.26	Parasite_single+time	6	7.38	Aspergillus+time	5	4.57
Copepod+Aspergillus	5	4.39	Copepod*time+Aspergillus	7	7.55	Parasite_single	5	5.04
Parasite_single	5	4.55	Null	3	8.07	Copepod+Aspergillus	5	5.1
Copepod*time	6	5.03	Parasite	4	9.15	Parasite_single*time	8	5.43
Copepod*Aspergillus	6	5.61	Copepod+Aspergillus+time	6	9.17	Parasite_single+time	6	6.06
Copepod*Asperigllus*time	10	5.6	Copepod*Aspergillus+time	7	9.38	Copepod*time	6	6.09
Aspergillus+time	5	5.68	Copepod	4	10	Copepod+Aspergillus+time	6	6.12
Copepod+Aspergillus+time	6	6.05	Aspergillus	4	10	Copepod*Aspergillus	6	7
Parasite_single+time	6	6.21	Parasite_single	5	10.3	Copepod*Asperigllus*time	10	7.03
Copepod*time+Aspergillus	7	7.02	Copepod+Aspergillus	5	12	Copepod*time+Aspergillus	7	7.94
Copepod*Aspergillus+time	7	7.27	Copepod*Aspergillus	6	12.3	Copepod*Aspergillus+time	7	8.02

Table S3.9: AIC Table of models for T5A expression in the laboratory experiment (random effect: time| colony) with the best model highlighted. No models were tested without time because it was the best random slope. The highlighted model is better than the null model (Chi Sq.= 14.108, P= 8.64E-04) and the Parasite*time model by the LRT (Chi Sq.= 2.01, P= 0.156).

Model	**Degrees of freedom**	**Delta AIC**
Parasite*time	8	0
Parasite+time	7	0.0112
Parasite_single+time	8	0.673
Parasite_single*time	10	2.18
Copepod*Aspergillus+time	9	2.65
Copepod*Aspergillus*time	12	5.20
Copepod*time+Aspergillus	9	9.17

Copepod*time	8	9.49
Copepod+Aspergillus+time	8	9.84
Copepod+time	7	10.0
Null	5	10.1
Aspergillus+time	7	10.6
Copepod+Aspergillus+time	9	11.7
Aspergillus*time	8	12.5

Table S3.10: The best model of Tachylectin 5A (T5A) included the general Parasite term (Parasite) and time.

Random effects:						
	Groups	**Name**	**Variance**	**Std.Dev.**	**Corr**	
	colony	(Intercept)	0.0244	0.156		
		time1	6.65E-03	0.0815	0.3	
	Residual		0.00523	0.0723		
Fixed effects:						
	Estimate	**Std. error**	**df**	**t value**	**Pr(>|t|)**	**95% CI**
(Intercept)	0.401	0.0530	8.14	7.56	6.0E-05	0.297-0.505
Parasite	0.0369	0.00984	53	3.75	4.4E-04	0.0176-0.0562
Time	0.0330	0.0285	8	1.16	0.280	-0.0228-0.0888

Table S3.11: AIC tables of models for IκB expression in the laboratory experiment. Two sets of models were tested with different random effects because Parasite and Parasite_single were both supported as random slopes. (a) Models with the random effect: Parasite| colony: Parasite*time is the best model by AIC, but the null model is best by the LRT (Chi Sq. = 2.01, P= 0.156). (b) Models with the random effect: Parasite_single | colony: the null model is the best model by AIC and parsimony.

(a)

Model	**Degrees of freedom**	**Delta AIC**
Parasite * time	8	0
Null	5	1.06
Parasite	6	1.69
Parasite + time	7	1.76

(b)

Model	Degrees of freedom	Delta AIC
Null	8	0
Parasite_single *time	13	1.20
Parasite_single	10	2.63
Parasite_single +time	11	2.70

Table S3.12: The best model of IκB gene expression by AIC (parasite *time), supports a trend for increasing expression in the presence of a parasite during the early time point only, though the null is the best model by the LRT (P=0.07).

	Estimate	Std. error	Degrees of freedom	t value	Pr(>|t|)
(Intercept)	0.261	0.0201	8	13.0	0.0000
Parasite	0.0178	0.0155	8	1.15	0.285
Time	-0.0153	0.00696	52	-2.20	0.0322
Parasite:time	0.0135	0.00696	52	1.94	0.0583

Table S3.13: AIC Table of models for MMP expression in the laboratory experiment (random effect: 1| colony) with the best model highlighted.

Model	Degrees of freedom	Delta AIC
Null	3	0
Copepod	4	1.021
Copepod * time	6	1.1756
Parasite * time	6	1.3558
Parasite	4	1.5652
Aspergillus	4	1.90
Copepod + time	5	2.25
Parasite + time	5	2.80
Copepod + Aspergillus	5	2.92
Copepod * time + Aspergillus	7	3.07
Aspergillus + time	5	3.14
Copepod + time + Aspergillus	6	4.15
Aspergillus * time	6	5.14
Copepod + Aspergillus * time	7	6.15
Copepod * Aspergillus * time	10	6.67

Table S3.14: Copepod severity in the laboratory experiment is not predicted by time, co-infection, or their interaction.

	Degrees of Freedom	**Delta AIC**	**AIC Weight**	**Cumulative Weight**
Null	3	0	0.64	0.64
Co-infection	4	1.5	0.3	0.95
2Coinfect*Time	6	5.01	0.05	1

Table S3.15: The AIC Table for MFPS prevalence with the best model highlighted.

	Degrees of freedom	**Delta AIC**	**AIC Weight**
Size^2 + temperature + coral cover	6	0	1
Coral cover + depth + temperature + size	6	75.2	0
null	2	164.32	0

Table S3.16: The best model of MFPS prevalence includes size^2 as a predictor.

Random effects							
	Groups	**Name**	**Variance**	**Std.Dev**			
	site	(Intercept)	0.290	0.538			
Fixed effects:					**95% CI**		
	Estimate	**Std. error**	**z value**	**Pr(>|z|)**	**Left**	**Right**	
(Intercept)	-0.683	0.156	-4.38	1.21E-05	-0.978	-0.377	
size	2.46	0.209	11.8	<2.00E-16	2.05	2.87	
I(size^2)	-1.13	0.154	-7.38	1.57E-13	-1.43	-0.833	
Temper-ature	-0.6465	0.2918	-2.216	0.0267	-1.22	-0.0747	
Coral cover	-0.3961	0.2345	-1.689	0.0911	-0.856	0.0634	

Table S3.17: The AIC Table for MFPS severity with the best model highlighted. Site was tested separately with each predictor due to convergence errors.

Model	**DF**	**Delta AIC**
Size^2+site	18	0
Size+site	17	4.41
Size^2+temperature	8	17.7
Size+temperature+copper	7	20.4
Size^2+coral cover	8	21.7

Size+coral cover+copper	7	24.6
Coral cover+site	17	32.3
Site	16	35.1
Null	2	57.0

Table S3.18: The summary of the best model for MFPS severity includes size^2 and site (Table S2) as predictors.

	Estimate	**Std Error**	**t value**	**Pr(>t)**	**95% CI**
(Intercept)	2.52	0.295	8.54	<2.00E-16	1.95, 3.10
Size	0.834	0.148	5.63	1.83E-08	0.543, 1.12
Size^2	-0.256	0.121	-2.11	0.0346	-0.493, -0.0185
SiteCB	-0.511	0.358	-1.428	0.153	-1.21, 0.191
SiteCH	0.015	0.334	0.043	0.965	-0.641, 0.670
SiteE	-0.709	0.349	-2.03	0.0424	-1.39, -0.0242
SiteF	-0.767	0.322	-2.38	0.0172	-1.40, -0.136
SiteG1	-0.0572	0.344	-0.166	0.868	-0.732, 0.617
SiteG2	-0.834	0.390	-2.14	0.0326	-1.60, -0.069
SiteL	0.0319	0.307	0.104	0.917	-0.570, 0.634
SiteM	-0.708	0.321	-2.21	0.0273	-1.34, -0.0793
SiteML	-0.615	0.337	-1.83	0.068	-1.27, 0.046
SiteP	-0.077	0.358	-0.214	0.830	-0.778, 0.625
SiteR	-0.299	0.355	-0.841	0.400	-0.994, 0.397
SiteSC	-0.907	0.379	-2.39	0.0168	-1.65, -0.163
SiteTC	-0.739	0.396	-1.86	0.0625	-1.52, 0.0385
SiteTM	-1.05	0.351	-2.99	0.0028	-1.74, -0.361
logSigma	-0.0008	0.0413	-0.0190	0.985	-0.0817, 0.0802

Table S3.19: The AIC Table for amoebocyte density in the field with the best model highlighted.

Model	**Degrees of freedom**	**Delta AIC**
Copepod + site + reproductive status + coral cover	20	0
Fungus*copepod+ sea fan density +site +temperature +coral cover +sex	23	4.38
Null	2	132.53

Table S3.20: Summary of the best model of field amoebocyte density

	Estimate	**Std. error**	**z value**	**Pr(>|z|)**	**Confidence interval**
(Intercept)	10.0	0.0498	202	<2.00E-16	9.94, 10.1
Copepod infection	0.0870	0.0139	6.28	3.47E-10	0.0597, 0.114
siteCB	-0.307	0.0745	-4.13	3.67E-05	-0.454, -0.160
siteCH	-0.277	0.0782	-3.54	0.000407	-0.431, -0.122
siteE	-0.441	0.0677	-6.51	7.56E-11	-0.575, -0.307
siteF	-0.107	0.0778	-1.37	0.170	-0.259, 0.0456
siteG1	0.153	0.0747	2.05	0.0407	0.0055, 0.300
siteG2	-0.264	0.0704	-3.75	0.000179	-0.402, -0.125
siteL	-0.157	0.0874	-1.80	0.0720	-0.329, 0.0153
siteM	0.0435	0.0746	0.583	0.560	-0.101, 0.188
siteML	-0.323	0.0724	-4.46	8.17E-06	-0.466, -0.18
siteP	-0.419	0.0667	-6.29	3.28E-10	-0.55, -0.288
siteR	-0.430	0.0692	-6.22	5.02E-10	-0.566, -0.295
siteSC	-0.269	0.0706	-3.81	0.000141	-0.408, -0.129
siteTC	-0.226	0.0752	-3.00	0.00269	-0.374, -0.0765
siteTM	-0.357	0.0685	-5.21	1.89E-07	-0.491, -0.223
coralcov	0.178	0.0448	3.97	7.18E-05	0.0891, 0.267
Reproductive status: M vs. F	0.00802	0.0175	0.457	0.647	-0.0265, 0.0426
Reproductive status: reproductive vs. not	0.0507	0.0106	4.77	1.84E-06	0.0298, 0.0715

CHAPTER 4

Figure S4.1: Map of survey sites in The Natural Reserve of La Parguera and in Guánica, on the southwest coast of Puerto Rico.

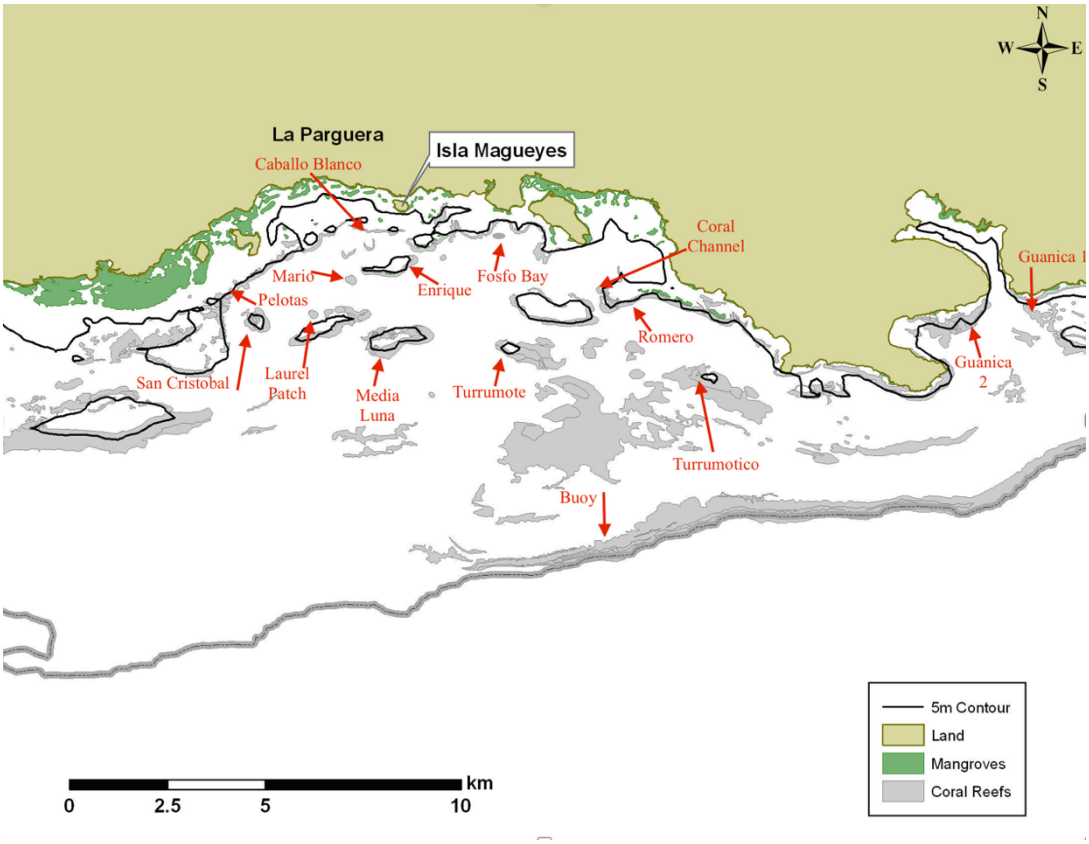

Table S4.1: GPS coordinates of sites in La Parguera, Puerto Rico with the type of temperature logger and the copper sediment concentration from Pait et al. (2007).

Reef site name and #	Latitude	Longitude	Temper-ature Logger	Copper sediment concentration range
Turrumotico (#1)	17° 55.743'	66° 58.487"	iButton	0.0-0.9 µg/g
Turrumote (#2)	17° 56.097'	67° 01.130"	HOBO	1.0-1.9 µg/g (Indicator Kriging, Fig. S4.2b)
Laurel Patch (#3)	17° 56.537'	67° 04.057'	iButton	0.0-0.9 µg/g
Media Luna (#4)	17° 56.096'	67° 02.911'	HOBO	2.0-4.1 µg/g
Pelotas (#5)	17° 57.446"	67° 04.183'	HOBO	2.0-4.1 µg/g
Caballo Blanco (#6)	17° 57.831'	67° 02.940'	iButton	2.0-4.1 µg/g
Enrique (#7)	17° 57.294'	67° 02.608'	HOBO	4.2-80.6 µg/g
Corral Channel (#8)	17° 56.959'	66° 59.938"	iButton	4.2-80.6 µg/g
Fosfo Bay (#9)	17° 57.544'	67° 00.826'	iButton	4.2-80.6 µg/g
Mario reef (#10)	17° 57.170'	67° 03 387'	HOBO	4.2-80.6 µg/g
Buoy (#11)	17° 53.291"	66° 59.884'	HOBO	0.0-0.9 µg/g (Indicator Kriging, Fig. S4.2b)
Romero (#12)	17° 56.830'	66° 59.431'	iButton	4.2-80.6 µg/g (Indicator Kriging, Fig. S4.2b)
San Cristobal (#13)	17° 56.497'	67° 04.497'	HOBO	1.0-1.9 µg/g (Indicator Kriging, Fig. S4.2b)
Guánica 1 (#14)	17° 56.862'	66° 54.087'	iButton	1.0-1.9 µg/g (Indicator Kriging, Fig. S4.2b)
Guánica 2 (#15)	17° 56.529'	66° 54.855'	iButton	1.0-1.9 µg/g

Figure S4.2: Figures from Pait et al. (2007) of copper sediment concentrations at the 15 study sites in La Parguera and Guánica Bay (see Table S1, above): (a) Sediment concentrations were obtained for 10 sites that were sampled by NOAA; (b) Indicator Kriging from Pait et al. (2007) was used to estimate concentrations at the five remaining sites. (Images courtesy of NOAA with permission, site numbers added; refer to Table 1 for site names matching numbers).

(a)

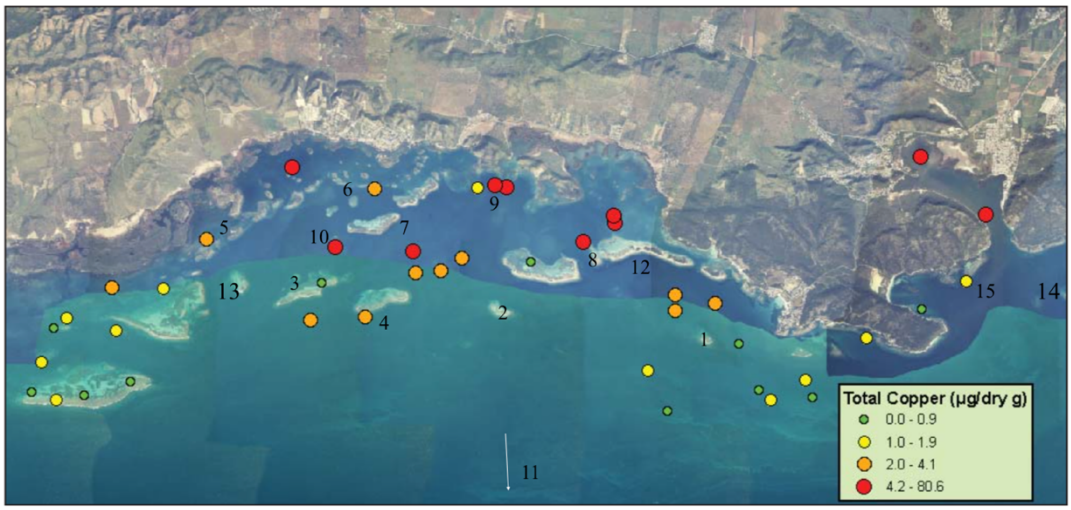

Figure 39. Map of copper detected in the sediments in southwest Puerto Rico. Data classified into quartiles.

(b)

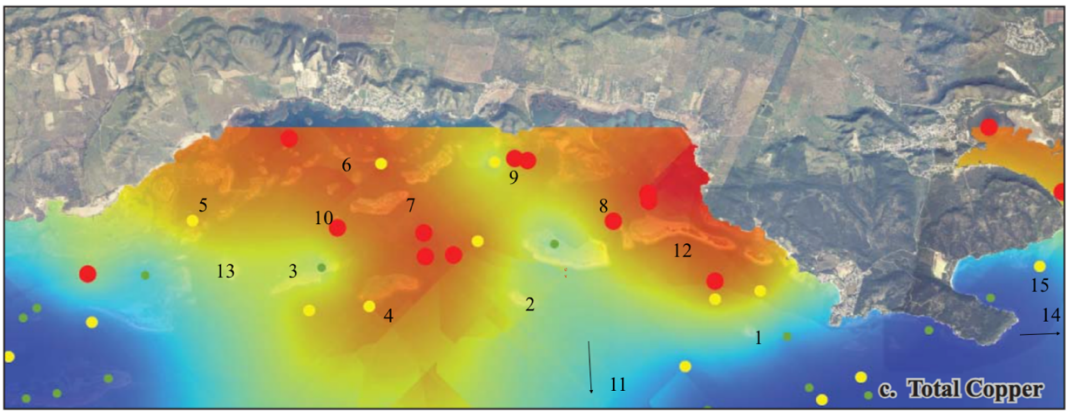

Figure 49. Indicator Kriging and measured concentrations of a) total PCBs, b) total DDTs, and c) copper. Colored dots represent sediment contaminant quantiles (●, low; ●, medium; ●, high).

Figure S4.3: (A) The clonally-replicated laboratory experiment was designed using 12 clippings from each of 10 sea fans. (B) The fully factorial experiment incorporated the clonal replicates to control for genotype and host identity in testing two temperatures (28°C and 30°C), three copper concentrations, and the live pathogen inoculation with the labyrinthulid in 2x3x2 design. (C) The timeline for the experiment ran from June 17 to June 23 with 1 day of acclimation and 5 days of experimental treatments.

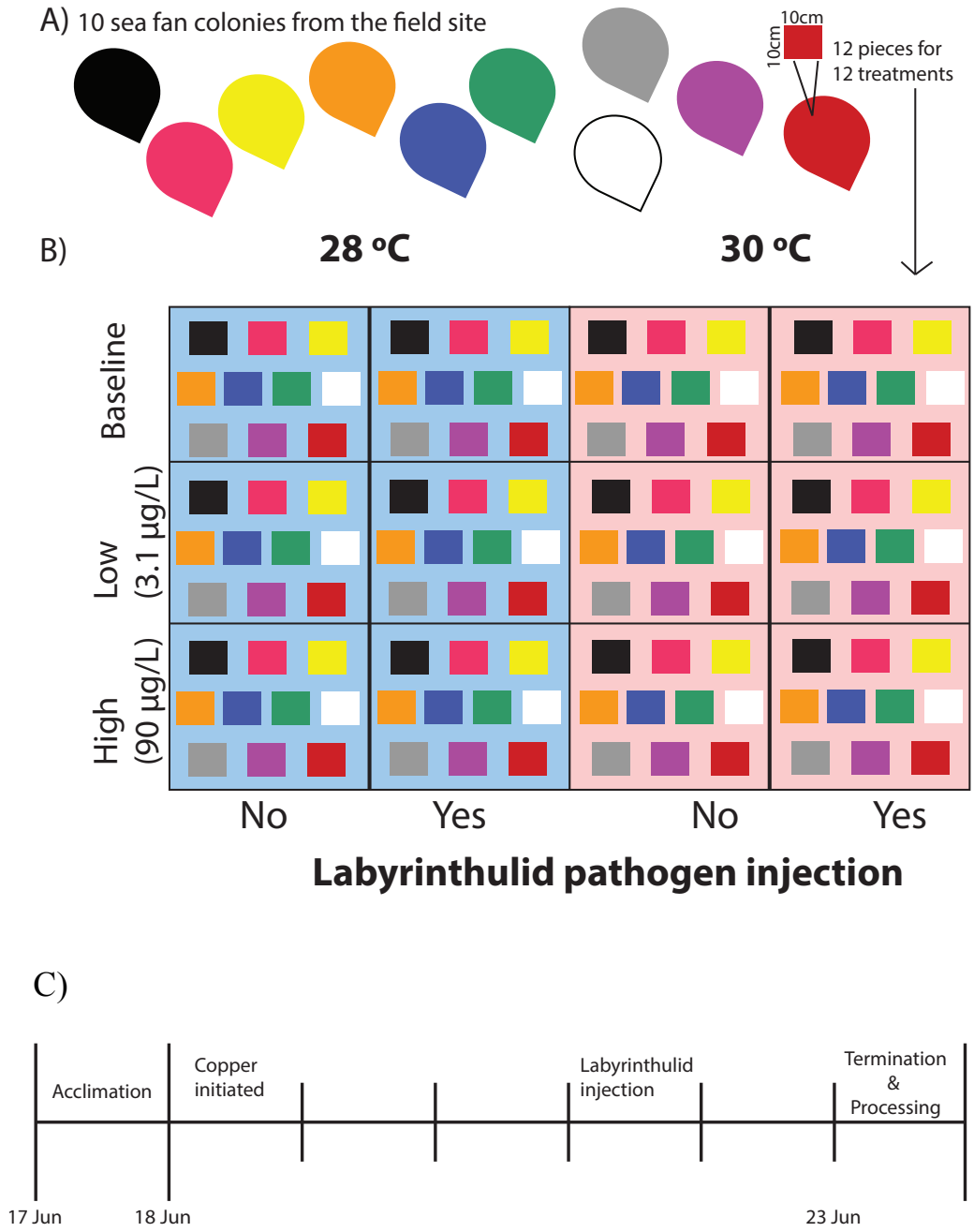

Figure S4.4: The 1st principal component of a suite of temperature metrics (overall minimum, overall maximum and monthly averages from May to November) is closely correlated with the average temperature across the time period.

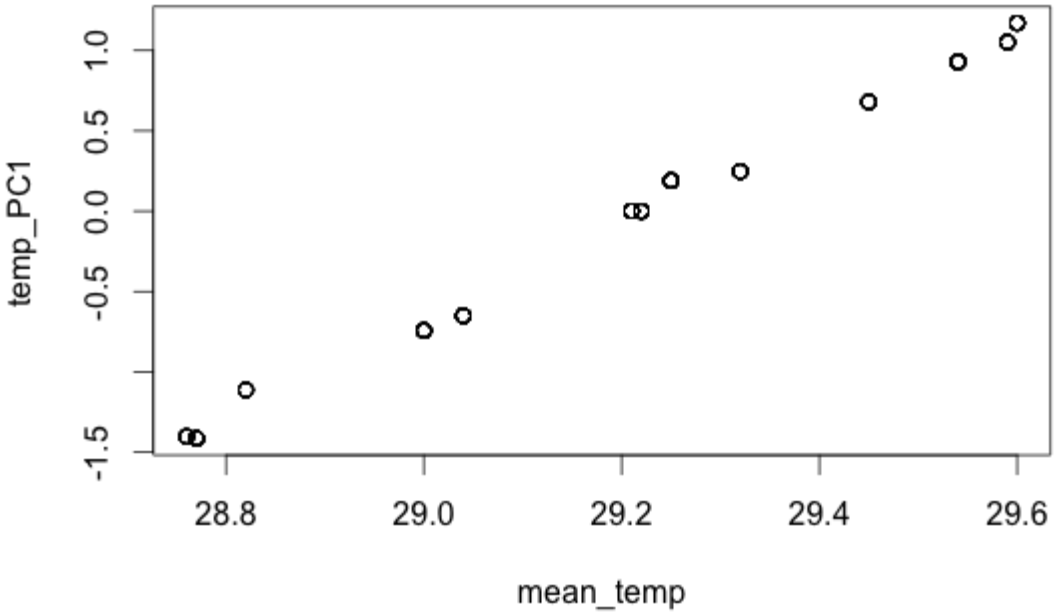

Figure S4.5: Amoebocyte densities cluster into two groups in the field data with densities at level 1 (0.0-0.9 µg/g) grouping separately from the three higher sediment copper levels (1.0-1.9 µg/g, 2.0-4.1 µg/g, 4.2-80.6 µg/g).

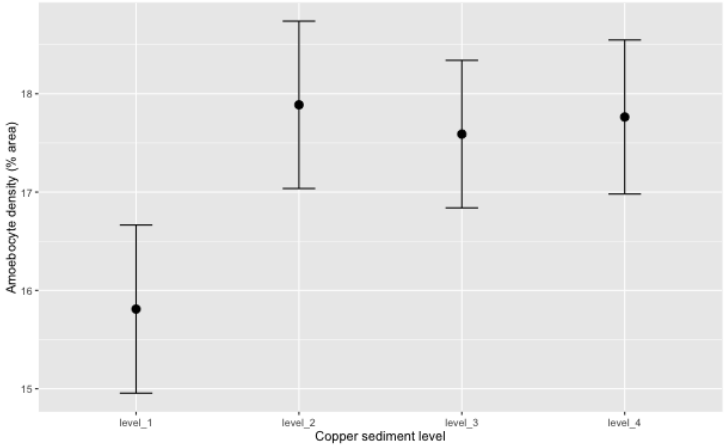

Figure S4.6: We tested copper as a predictor in four levels as well as two levels for models of incidence and recovery based on exploratory plots indicating that (a) levels 2 through 4 group together for incidence and (b) levels 1 through 3 group together for recovery.

(a) (b)

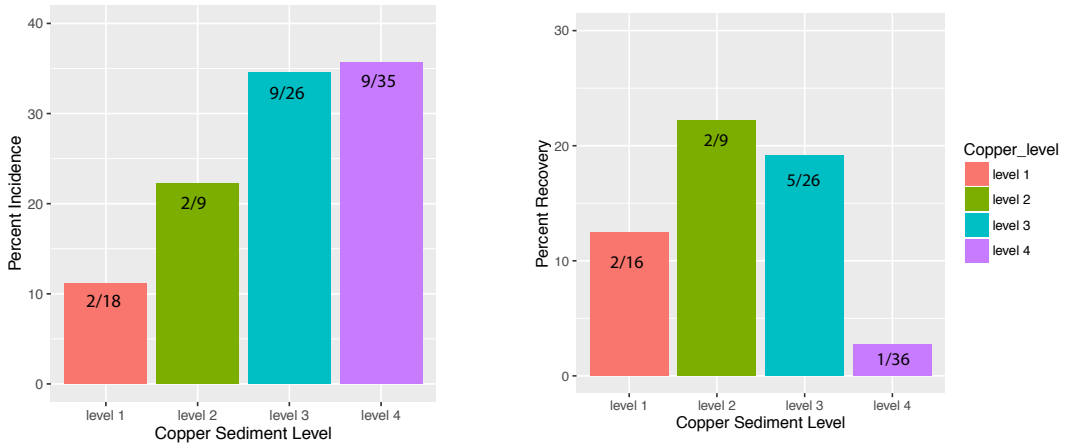

Table S4.2: AIC Table for amoebocyte density in the field (GLMM with negative binomial distribution and colony as a random effect): The model with copper sediment concentration, sea fan density, and infection status is the best model by AIC and parsimony (in green).

Model	**Number of estimated parameters**	**Delta_AIC**	**AIC Weight**
Copper (two groups) + depth + sea fan density + infection status	9	0	0.97
Infection status + depth	7	7.26	0.03
Temperature + copper (two groups)	6	13.57	0
Null	3	13.8	0

Table S4.3: Summary of best model of field amoebocyte density: **Copper (2 groups) + depth + sea fan density + infection status.**

	Estimate	**Std. error**	**z value**	**Pr(>|z|)**	**Confidence Interval**	
(Intercept)	5.19	0.0432	120	<2.00E-16	5.11	5.28
Infection_status_1 (Co-infection vs. copepod)	-0.030	0.0385	-0.78	0.436	-0.0455	0.0106
Infection_status_2 (Coinfection vs. labyrinthulid)	-0.120	0.0460	-2.61	0.00892	0.0301	0.210
Infection_status_3 (Coinfection vs. neither)	0.0425	0.0379	1.12	0.262	-0.268	0.0521
Sea fan density	-0.0804	0.0494	-1.63	0.1032	-0.177	0.0163
Depth	0.148	0.0570	2.6	0.00938	0.0364	0.0260

Table S4.4: Multiple comparisons of infection status as a predictor of amoebocyte density in the field for best model.

	Estimate	**Std. error**	**z value**	**Pr(>|z|)**	**Confidence interval**	
Labyrinthulid vs. Copepod	0.0902	0.0619	1.46	0.433	-0.0651	0.246
Co-infection vs. Copepod	-0.138	0.113	-1.22	0.589	-0.422	0.147
Neither vs. Copepod	-0.0726	0.0308	-2.36	0.0735	-0.150	0.00461
Co-infection vs. Labyrinthulid	-0.228	0.112	-2.03	0.158	-0.510	0.0540
Neither vs. Labyrinthulid	-0.163	0.0606	-2.69	0.0306 *	-0.315	-0.0108
Neither vs. Co-infection	0.0652	0.113	0.576	0.932	-0.219	0.349

Table S4.5: The AIC table for MFPS disease recovery including all models better than the null by AIC (GLM with binomial distribution): the model with copper alone is the best model by AIC and parsimony, and significantly better than the null model by the likelihood ratio test (in gray).

Model	**Number of estimated parameters**	**ΔAIC**	**AIC Weight**
Copper (2 groups)	2	0	0.48
Copper (2 groups) * temperature	4	0.95	0.3
Copper (4 groups) * temperature	7	3.24	0.09
Null	1	3.4	0.09
Coral cover + sea fan density + temperature + depth	5	4.94	0.04

Table S4.6: MFPS disease recovery is best predicted by copper, but not significantly.

	Estimate	**Std. error**	**z value**	**Pr(>|z|)**	**Confidence interval**
(Intercept)	-3.56	1.01	-3.51	0.000456*	-6.43, -2.02
Copper (3 low together)	2.02	1.08	1.87	0.0618	0.274, 4.95

Table S4.7: The AIC table for MFPS disease incidence (GLM with binomial distribution). Copper alone is the best predictor by AIC and parsimony. Models with copper/temperature interactions are not includd due to high variance inflation factors. (No models are significantly better than the null (likelihood ratio test).

	Number of estimated parameters	**ΔAIC**	**AIC Weight**
Copper (2 groups)	2	0	0.43
Null	1	0.66	0.31
Sea fan density	2	1.04	0.26

Table S4.8: MFPS disease incidence is best predicted by copper, but not significantly.

	Estimate	**Std. error**	**Adjusted SE**	**z value**	**Confidence interval**
(Intercept)	-2.08	0.75	-2.77	0.00556	-3.94, -0.823
Copper_binary	1.16	0.795	1.46	0.144	-0.212, 3.06

Table S4.9: The AIC table for labyrinthulid disease prevalence including all models with non-zero weights, Buoy site excluded (GLM with binomial distribution): the model with depth and mean temperature is the best by AIC and parsimony (in gray), and significantly better than the null model by the likelihood ratio test (Chi-squared statistic= 10.9, P = 4.25E-03, LRT). **Model**	**K**	**ΔAIC**	**AIC Weight**
Temperature + depth	3	0	0.75
Copper* temperature + sex +copepod	11	2.41	0.23
Null	1	6.92	0.02

Table S4.10: Summary of best model of labyrinthulid prevalence in the field, Buoy site excluded.

	Estimate	**Std. error**	**z value**	**Pr(>|z|)**	**Confidence Interval**	
(Intercept)	-2.64	0.545	-4.85	1.25E-06	-3.94	-1.74
Temperature	-1.22	0.770	-1.59	0.113	-2.84	0.255
Depth	2.51	1.03	2.42	0.0154	0.708	4.83

Figure S4.7: Labyrinthulid prevalence increased with depth.

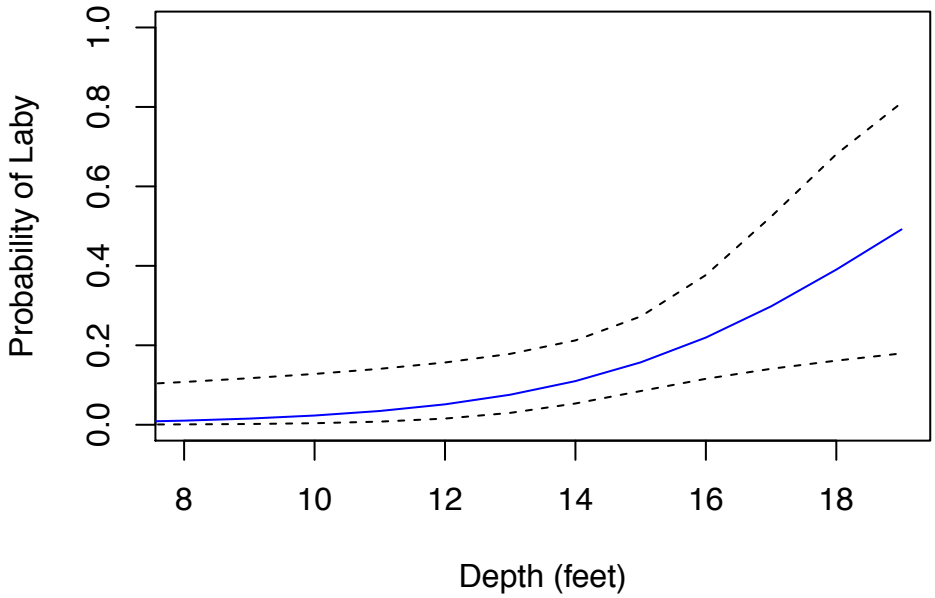

Table S4.11: The AIC table for copepod disease prevalence including all models with non-zero weights (GLMM with binomial distribution and site as a random effect): no models are better than the null.

Model	**Number of estimated parameters**	**ΔAIC**	**AIC Weight**
Null	2	0	0.31
Sex	4	0.03	0.3
Size * labyrinthulid	5	1.27	0.16
Depth * labyrinthulid + sex	7	3.84	0.04
Temperature * depth + sex	7	4.46	0.03
Size * sea fan density + sex	7	4.79	0.03
Size * depth + sex	7	5.01	0.03
Sea fan density^2 + labyrinthulid + coral cover + sex	8	5.53	0.02
Sea fan density * labyrinthulid + coral cover + sex	8	5.97	0.02
Size * coral cover + sex + labyrinthulid	8	6	0.02
Coral cover * temperature + labyrinthulid + sea fan density + sex	9	7.31	0.01
Size^2 + sea fan density + labyrinthulid + sex + coral cover	9	7.63	0.01
Sea fan density * depth + coral cover + sex + labyrinthulid	9	7.93	0.01
Coral cover * depth + sea fan density + sex + labyrinthulid	9	7.96	0.01
Coral cover * labyrinthulid + sea fan density + sex + temperature	9	7.96	0.01
Temperature * labyrinthulid + size + copper + coral cover + sea fan density + sex + depth	9	8	0.01
Coral cover^2 + temperature + sea fan density + sex + labyrinthulid	9	8.02	0.01

Table S4.12: Copepod infection is positively predicted by MFPS, which is better than the null model (Chi-square statistic = 42.3, P= 7.66E-11, likelihood ratio test).

	Estimate	**Std. error**	**z value**	**Pr(>|z|)**	**Confidence interval**
(Intercept)	-2.56	0.599	-4.28	1.86E-05*	-3.74, -1.39

MFPS	3.45	0.678	5.09	3.56E-07*	2.12, 4.78

Table S4.13: The AIC table for MFPS prevalence including all models with non-zero weights (GLMM with binomial distribution and transect nested within site as a random effect): a quadratic model with size is the best model by AIC and parsimony (in green), and significantly better than the null (Chi-squared statistic = 118, P < 2.2E-16, likelihood ratio test).

Model	**Number of estimated parameters**	**ΔAIC**	**AIC Weight**
Size^2	5	0	0.47
Size^2 + copper	8	0.75	0.33
Size^2 + copper + depth	9	1.81	0.19
Size^2 + copper + depth + coral cover + sea fan density + temperature	12	7.55	0.01
Null	3	114	0

Table S4.14: MFPS prevalence is best predicted by size, with a quadratic term indicating a decline in the largest sea fans.

	Estimate	**Std. error**	**z value**	**Pr(>|z|)**	**Confidence interval**
(Intercept)	-0.304	0.142	-2.14	0.0321*	-0.582, -0.0260
Size	2.08	0.207	10.1	<2.00E-16*	1.67, 2.48
Size ^2 (quadratic)	-1.01	0.152	-6.65	2.94E-11*	-1.31, -0.713

Figure S4.8: MFPS is best predicted by the quadratic term for size, i.e. prevalence increases with size, but decreases in the largest sea fans.

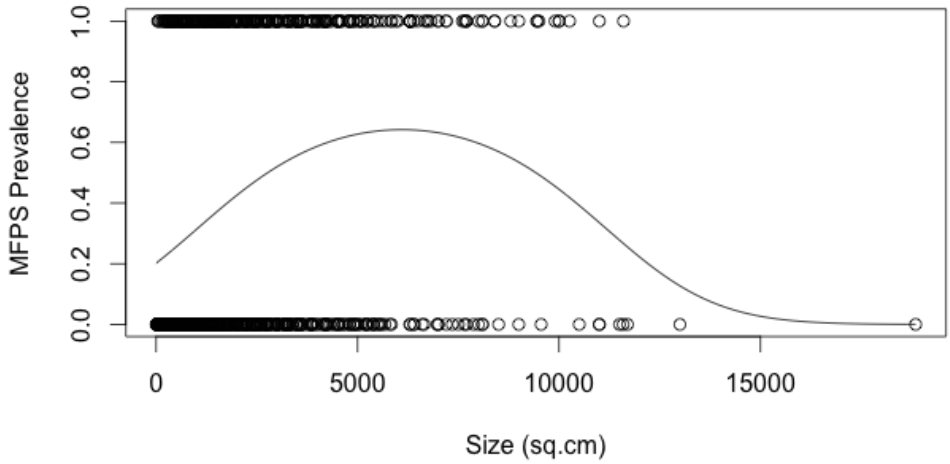

Table S4.15: The AIC table for models of MFPS severity within 5 AIC units (censored regression): the model with the interaction of size and temperature and an additive effect of copper is the best model by the combination of AIC and parsimony (in green) with several models within 2 AIC. It is also significantly better than the null (Chi-squared statistic = 85.9, P < 2.2e-16, likelihood ratio test).

Model	**ΔAIC**	**Degrees of freedom**
Depth^2 + Coral cover + copper + sea fan density + size + temperature	0	11
Temperature * coral cover + copper + sea fan density + size + depth	0.173	11
Temperature * copper + sea fan density + coral cover + size	0.876	12
Size * temp + copper	1.533	8
Temperature* copper + sea fan density + coral cover + size + depth	2.672	13
Size * temperature + copper + depth	2.773	9
Size * temperature + copper + depth + coral cover	3.727	10
Depth * copper + temperature + size	4.382	11
Temperature * sea fan density + copper + size + depth	4.408	10
Size * depth + temperature + copper	4.836	9
Null	75.461	2

Table S4.16: Best model of MFPS severity by AIC and parsimony.

	Estimate	**Std. error**	**t value**	**Pr(>t)**	**Confidence interval**
(Intercept)	1.89E+00	1.22E-01	15.5	< 2.00E-16*	1.65, 2.13
Size	1.55E-04	2.37E-05	6.54	6.13E-11*	1.08E-04, 2.01E-04
Temp. PC1	-5.24E-01	1.18E-01	-4.43	9.25E-06*	-7.55E-01, 0.292E-01
Copper level2	-3.56E-01	1.55E-01	-2.30	0.0215*	-6.60E-01, -5.25E-02
Copper level3	-8.73E-02	1.89E-01	-0.463	0.644	-4.57E-01, 2.83E-01
Copper level4	-6.08E-03	1.54E-01	-0.04	0.968	-3.07E-01, 2.95E-01
Size * temp. PC1	7.70E-05	2.95E-05	2.61	0.00912 *	1.91E-05, 1.35E-04
logSigma	3.15E-02	3.77E-02	0.834	0.404	-4.25E-02, 1.05E-01

Figure S4.9: Increasing temperatures (a) increase MFPS severity in larger colonies while decreasing MFPS severity in small colonies; (b) Increasing temperature also exacerbates the increase in MFPS severity with colony size (Figures use scaled variables as in censReg models).

(a) (b)

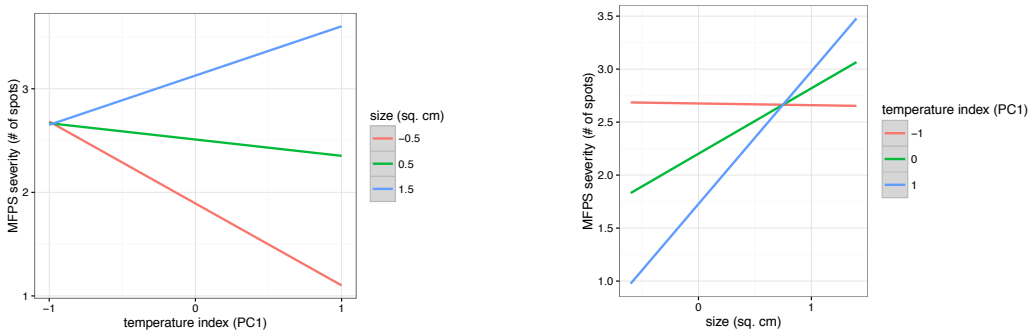

Table S4.17: AIC table of laboratory amoebocyte density models (LMM with colony nested within table as a random effect): the 3-way interaction between copper, temperature and labyrinthulid best predicts amoebocyte density (in green).

Model	**Number of estimated parameters**	**ΔAIC**	**AIC Weight**
Copper* temperature * labyrinthulid	15	0	0.82
Temperature * labyrinthulid	7	4.87	0.07
Copper * temperature	9	6.8	0.03
Copper * temperature + labyrinthulid	10	6.9	0.03
Temperature * labyrinthulid +copper	9	7.71	0.02
Copper* labyrinthulid + temperature	10	8.08	0.01
Temperature	5	8.83	0.01
Labyrinthulid + temperature	6	9.01	0.01
Null model	4	11.37	0

Table S4.18: Summary of pairwise comparisons using lsmeans, sorted by significance, for the best model of amoebocyte density in the laboratory experiment. The three comparisons that differ from the control are highlighted in green.

Contrast	Estimate	Standard error	Degrees of freedom	t ratio	P value
low temp,base_Cu,no_Laby - high temp,base_Cu,Laby	-0.219	0.0541	382	-4.05	0.0041
high temp,base_Cu,Laby – low temp,low_Cu,Laby	0.200	0.0532	381	3.76	0.0066
high temp,low_Cu,no_Laby – high temp,base_Cu,Laby	-0.181	0.0533	382	-3.39	0.014
low temp,base_Cu,Laby – high temp,base_Cu,Laby	-0.182	0.0540	381	-3.36	0.014
low temp,base_Cu,no_Laby – high temp,low_Cu,Laby	-0.177	0.0551	381	-3.22	0.0186
high temp,base_Cu,no_Laby - high temp,base_Cu,Laby	-0.157	0.0529	382	-2.98	0.0292
high temp,base_Cu,Laby - high temp,hi_Cu,Laby	0.163	0.0545	381	2.99	0.0292
low temp,low_Cu,Laby - high temp,low_Cu,Laby	-0.158	0.0543	381	-2.91	0.0316
low temp,low_Cu,no_Laby - high temp,base_Cu,Laby	-0.148	0.0528	381	-2.80	0.0391
low temp,base_Cu,no_Laby - low temp,hi_Cu,no_Laby	-0.151	0.0548	381	-2.761	0.0399
high temp,low_Cu,no_Laby - high temp,low_Cu,Laby	-0.139	0.0543	381	-2.56	0.0635
low temp,base_Cu,Laby - high temp,low_Cu,Laby	-0.140	0.0552	381	-2.54	0.0635
low temp,hi_Cu,no_Laby - low temp,low_Cu,Laby	0.132	0.0539	381	2.45	0.0758
high temp,base_Cu,Laby - low temp,hi_Cu,Laby	0.124	0.0550	381	2.25	0.119
high temp,base_Cu,no_Laby - high temp,low_Cu,Laby	-0.116	0.0540	382	-2.14	0.128
high temp,hi_Cu,no_Laby - high temp,base_Cu,Laby	-0.112	0.0525	382	-2.141	0.128
high temp,low_Cu,Laby - high temp,hi_Cu,Laby	0.121	0.0556	381	2.181	0.128

high temp,low_Cu,no_Laby - low temp,hi_Cu,no_Laby	-0.113	0.0540	382	-2.092	0.133
low temp,hi_Cu,no_Laby - low temp,base_Cu,Laby	0.114	0.0547	381	2.08	0.133
low temp,base_Cu,no_Laby - high temp,hi_Cu,no_Laby	-0.107	0.0540	381	-1.97	0.156
low temp,low_Cu,no_Laby - high temp,low_Cu,Laby	-0.106	0.0540	382	-1.970	0.156
low temp,hi_Cu,no_Laby - high temp,hi_Cu,Laby	0.0951	0.0552	381	1.72	0.258
low temp,base_Cu,no_Laby - low temp,hi_Cu,Laby	-0.0954	0.0565	381	-1.69	0.262
high temp,base_Cu,no_Laby - low temp,hi_Cu,no_Laby	-0.0896	0.0535	381	-1.67	0.262
high temp,hi_Cu,no_Laby - low temp,low_Cu,Laby	0.0873	0.0533	382	1.64	0.270
low temp,low_Cu,no_Laby - low temp,hi_Cu,no_Laby	-0.0802	0.0535	381	-1.50	0.343
high temp,low_Cu,Laby - low temp,hi_Cu,Laby	0.0820	0.0561	381	1.46	0.353
low temp,low_Cu,Laby - low temp,hi_Cu,Laby	-0.0761	0.0557	381	-1.37	0.407
low temp,base_Cu,no_Laby - low temp,low_Cu,no_Laby	-0.0710	0.0544	381	-1.31	0.407
high temp,low_Cu,no_Laby - high temp,hi_Cu,no_Laby	-0.0683	0.0532	381	-1.28	0.407
low temp,hi_Cu,no_Laby - high temp,base_Cu,Laby	-0.0677	0.0532	381	-1.27	0.407
high temp,hi_Cu,no_Laby - low temp,base_Cu,Laby	0.0692	0.0540	381	1.28	0.407
high temp,hi_Cu,no_Laby - high temp,low_Cu,Laby	-0.0708	0.0536	381	-1.32	0.407
low temp,base_Cu,no_Laby - high temp,base_Cu,no_Laby	-0.0616	0.0544	381	-1.13	0.501
low temp,base_Cu,no_Laby - high temp,hi_Cu,Laby	-0.0561	0.0560	381	-1.00	0.550
high temp,low_Cu,no_Laby - low temp,hi_Cu,Laby	-0.0571	0.0557	381	-1.03	0.550

low temp,hi_Cu,no_Laby - low temp,hi_Cu,Laby	0.0558	0.0557	381	1.00	0.550
low temp,base_Cu,Laby - low temp,hi_Cu,Laby	-0.0581	0.0565	381	-1.028	0.550
low temp,low_Cu,no_Laby - low temp,low_Cu,Laby	0.0517	0.0536	381	0.966	0.566
high temp,hi_Cu,no_Laby - high temp,hi_Cu,Laby	0.0504	0.0545	381	0.926	0.586
high temp,base_Cu,no_Laby - high temp,hi_Cu,no_Laby	-0.0450	0.0528	381	-0.852	0.631
low temp,hi_Cu,no_Laby - high temp,hi_Cu,no_Laby	0.0446	0.0532	381	0.84	0.631
high temp,base_Cu,no_Laby - low temp,low_Cu,Laby	0.0423	0.0536	382	0.789	0.658
high temp,base_Cu,Laby - high temp,low_Cu,Laby	0.0416	0.0536	382	0.775	0.658
low temp,base_Cu,no_Laby - high temp,low_Cu,no_Laby	-0.0382	0.0548	381	-0.698	0.680
low temp,base_Cu,no_Laby - low temp,base_Cu,Laby	-0.0373	0.0556	381	-0.672	0.680
low temp,low_Cu,no_Laby - high temp,hi_Cu,no_Laby	-0.0355	0.0528	381	-0.673	0.680
low temp,low_Cu,Laby - high temp,hi_Cu,Laby	-0.0368	0.0552	381	-0.667	0.680
low temp,hi_Cu,Laby - high temp,hi_Cu,Laby	0.0393	0.0569	381	0.69	0.680
high temp,base_Cu,no_Laby - low temp,hi_Cu,Laby	-0.0338	0.0553	381	-0.611	0.688
low temp,low_Cu,no_Laby - high temp,low_Cu,no_Laby	0.0328	0.0537	381	0.61	0.688
low temp,low_Cu,no_Laby - low temp,base_Cu,Laby	0.0337	0.0544	381	0.62	0.688
high temp,base_Cu,no_Laby - high temp,low_Cu,no_Laby	0.0233	0.0536	382	0.435	0.782
high temp,base_Cu,no_Laby - low temp,base_Cu,Laby	0.0243	0.0544	381	0.446	0.782
low temp,low_Cu,no_Laby - low temp,hi_Cu,Laby	-0.0244	0.0553	381	-0.441	0.782

low temp,hi_Cu,no_Laby - high temp,low_Cu,Laby	-0.0262	0.0543	381	-0.482	0.782
low temp,base_Cu,no_Laby - low temp,low_Cu,Laby	-0.0193	0.0548	381	-0.352	0.808
high temp,low_Cu,no_Laby - low temp,low_Cu,Laby	0.0190	0.0540	382	0.351	0.808
high temp,low_Cu,no_Laby - high temp,hi_Cu,Laby	-0.0179	0.0552	381	-0.323	0.808
low temp,base_Cu,Laby - low temp,low_Cu,Laby	0.0181	0.0547	381	0.33	0.808
low temp,base_Cu,Laby - high temp,hi_Cu,Laby	-0.0188	0.0560	381	-0.335	0.808
low temp,low_Cu,no_Laby - high temp,hi_Cu,Laby	0.0149	0.0548	381	0.272	0.837
high temp,hi_Cu,no_Laby - low temp,hi_Cu,Laby	0.0111	0.0549	381	0.203	0.879
high temp,base_Cu,no_Laby - low temp,low_Cu,no_Laby	-0.00944	0.0532	381	-0.178	0.886
high temp,base_Cu,no_Laby - high temp,hi_Cu,Laby	0.00547	0.0548	381	0.1	0.935
high temp,low_Cu,no_Laby - low temp,base_Cu,Laby	0.000919	0.0549	382	0.017	0.987

Table S4.19: The AIC table for tissue damage including all models tested (GLM with Poisson distribution): the model with a temperature-copper interaction is the best model by AIC (in green), and significantly better than the null (Chi-squared = 40.4, P = 1.24E-07, likelihood ratio test).

Model	**Number of estimated parameters**	**ΔAIC**	**AIC Weight**
Temperature * copper	6	0	0.92
Copper + labyrinthulid + temperature	5	6.38	0.04
Temperature * labyrinthulid + copper	6	8.1	0.02
Labyrinthulid * copper * temperature	12	8.14	0.02
Labyrinthulid * copper + temperature	7	9.05	0.01
Null	1	30.41	0

Table S4.20: Summary of best model of 5-day integrative metric of tissue damage.

	Estimate	**Std. Error**	**z value**	**Pr(>|z|)**
(Intercept)	0.931	0.210	4.44	9.04E-06
Temperature	0.905	0.240	3.77	0.000166*
Copper: high vs. base	1.05	0.236	4.46	8.17E-06*
Copper: low vs. base	-0.931	0.358	-2.61	0.00909*
Temperature: copper high vs. base	-0.807	0.282	-2.86	0.00427*
Temperature: copper low vs. base	0.542	0.401	1.35	0.177

Table S4.21: Results for compact letter display ("cld") for laboratory tissue damage.

Treatment	**lsmean**	**Standard error**	**Group for plot**
Low temperature, base copper	8.11E-01	0.333	ab
Low temperature, low copper	1.61E-10	0.500	a
Low temperature, high copper	1.98E+00	0.186	c
High temperature, base copper	1.98E+00	0.186	c
High temperature, low copper	1.45E+00	0.243	bc
High temperature, high copper	2.08E+00	0.177	c